

Evaluating the Robustness of Trigger Set-Based Watermarks Embedded in Deep Neural Networks

Suyoung Lee¹, Wonho Song¹, Suman Jana², Meeyoung Cha¹, Sooel Son¹

¹*School of Computing, KAIST*

²*Columbia University*

Abstract

Trigger set-based watermarking schemes have gained emerging attention as they provide a means to prove ownership for deep neural network model owners. In this paper, we argue that state-of-the-art trigger set-based watermarking algorithms do not achieve their designed goal of proving ownership. We posit that this impaired capability stems from two common experimental flaws that the existing research practice has committed when evaluating the robustness of watermarking algorithms: (1) incomplete adversarial evaluation and (2) overlooked adaptive attacks.

We conduct a comprehensive adversarial evaluation of 10 representative watermarking schemes against six of the existing attacks and demonstrate that each of these watermarking schemes lacks robustness against at least two attacks. We also propose novel adaptive attacks that harness the adversary’s knowledge of the underlying watermarking algorithm of a target model. We demonstrate that the proposed attacks effectively break all of the 10 watermarking schemes, consequently allowing adversaries to obscure the ownership of any watermarked model. We encourage follow-up studies to consider our guidelines when evaluating the robustness of their watermarking schemes via conducting comprehensive adversarial evaluation that include our adaptive attacks to demonstrate a meaningful upper bound of watermark robustness.

1 Introduction

The recent advent of deep neural networks (DNNs) has accelerated the development and application of diverse DNN models across various domains, including image search [23, 55], security [58, 59], finance [18, 20], and self-driving vehicles [52]. As machine learning technology evolves, the structures of state-of-the-art DNN models have become more complicated. This trend renders corporations with fewer computational resources unable to train state-of-the-art DNN models from scratch. For instance, the ImageNet [45] dataset holds 14M images; training a high-performing DNN model such

as a ResNet-50 [26], which consists of over 25M parameters, takes up to several weeks with a machine equipped a Tesla M40 GPU. Moreover, it is difficult to obtain a large number of high-quality training instances pertaining to privacy-sensitive information, thus rendering it infeasible for corporations with limited data access to produce a superb model.

An adversary may attempt to steal such a superb model and host another service that imitates the service provided by the original model. This adversary poses a grave threat to the model owner, who has invested resources and time to develop a high-performing model. DNN model theft thus infringes on the intellectual property (IP) of the model owner and discloses the owner’s business secrets. Accordingly, corporations seek a mechanism that proves the ownership of their DNN models to protect their IPs and business secrets.

Previous studies have proposed novel methods that validate ownership of a given DNN model, thus protecting the owner’s IP. Similar to watermarking algorithms devised to protect the IP of multimedia content, such as images and videos [31, 49], previous studies have proposed new ways of embedding watermarks into a given DNN model as well as algorithms that verify ownership [3, 11, 19, 25, 33, 36, 38, 44, 54, 61, 62]. The proposed watermarking algorithms are categorized into two types based on their methods of embedding watermarks: feature-based and trigger set-based methods.

Feature-based schemes [11, 44, 54] require white-box access to a model’s internal weight parameters. On the other hand, trigger set-based watermarking methods [3, 19, 25, 33, 36, 38, 61, 62] have gained attention due to their comparative merits of requiring black-box access for ownership verification. Trigger set-based schemes harness the common query interface of a suspect model. Specifically, these watermarking methods leverage carefully created images, called *key images*, as training instances. A model owner then assigns an arbitrary label, called a *target label*, to the key images and generates a *trigger set* that consists of an arbitrary number of key image and target label pairs. The owner trains a model on this trigger set as well as on the normal training data. When verifying ownership, the model owner queries the model in doubt

with the key images and checks whether the model returns the target label; this enables the model owner to verify ownership by using remote queries. Previous trigger set-based methods [3, 19, 25, 33, 36, 38, 61, 62] have in common that they use key images and target labels but differ in how they generate key images or select target labels.

Contributions. In this paper, we argue that trigger set-based watermarking methods today [3, 19, 25, 33, 36, 38, 61, 62] do not achieve their goal of enabling model owners to prove their ownership of watermarked DNN models. We believe that previous studies have not evaluated the robustness of their watermarking algorithms to the fullest extent, thereby failing to demonstrate their readiness for real-world deployment.

There exist two different strategies for evaluating the robustness of a DNN model: (1) proving a theoretical lower bound with approximation [4, 27] and (2) demonstrating an upper bound via adversarial evaluation with strong attacks. Previous watermarking studies [3, 19, 25, 33, 36, 38, 61, 62] have taken the latter approach, demonstrating their robustness against selected attacks. However, in performing adversarial evaluation, we observed two common flaws in previous studies when evaluating the robustness of their trigger set-based watermarking algorithms: (1) performing incomplete adversarial evaluation and (2) overlooking an adaptive adversary.

Incomplete adversarial evaluation. Because various attacks have been introduced across diverse studies in various contexts, we first consolidate and reorganize six existing attacks. We then categorize the existing attacks into two types, each of which corresponds to either of adversary’s two strategies: (1) claiming of ownership by the adversary or (2) obscuring the owner’s ownership.

We observed that no previous watermarking studies have considered the complete set of the existing strong attacks in their adversarial evaluation; thus, none has demonstrated their robustness against at least three critical attacks. Furthermore, we contend that adversarial evaluation of attacks employing the adversary’s first strategy (claiming of ownership by the adversary) is unnecessary. This strategy permits for a target model to contain watermarks from its original owner as well as the adversary, which demands additional proof to prove the adversary’s ownership (§5.3.1). Therefore, there is no motive for the adversary to employ this strategy alone unless she combines the two aforementioned strategies by obscuring the original watermarks and then injecting her own watermarks.

To this end, we perform our own adversarial evaluation against 10 of the representative trigger set-based watermarking schemes while taking into account the aforementioned problems. We demonstrate that they are weak against at least two of these attacks [35, 53, 61]. In particular, nine out of the 10 evaluated schemes were vulnerable to model stealing [39, 53] and evasion attacks [33, 35, 38].

Overlooked adaptive adversary. Previous studies focused on evaluating their watermark robustness against selected existing attacks. Meanwhile, a vast volume of recent research

on establishing the robustness of DNN models has considered adaptive adversaries [5, 7, 14, 28, 42, 47].

To this end, we propose novel attacks that a strong adaptive adversary is able to conduct. Under the assumption that this adversary knows the underlying watermarking algorithm of a target model, we demonstrate that the proposed adaptive attacks effectively enable the adversary to obscure the ownership of a target model, regardless of its underlying watermarking scheme. Therefore, our proposed attacks contribute to demonstrating a new upper bound of watermark robustness.

Overall, our experimental results demonstrate that trigger set-based watermarking schemes today are far from ready for real-world deployment. We recommend that future research evaluate their watermarking methods against at least all existing strong attacks, including our adaptive attacks, and consider our guidelines when demonstrating their watermark robustness via adversarial evaluation (§8).

In summary, this paper makes the following contributions:

1. We identify shortcomings in the current practice of conducting adversarial evaluation: incomplete adversarial evaluation and overlooked adaptive attacks.
2. We empirically demonstrate that at least two of the existing attacks breaks state-of-the-art trigger set-based watermarking algorithms and posit that this impaired capability stems from an experimental flaw of performing incomplete adversarial evaluation.
3. We propose novel adaptive attacks and encourage for follow-up studies to consider our adaptive attacks when demonstrating watermark robustness.
4. We suggest guidelines for evaluating the robustness of trigger set-based DNN watermarking algorithms.

2 Background

2.1 DNN Ownership Verification

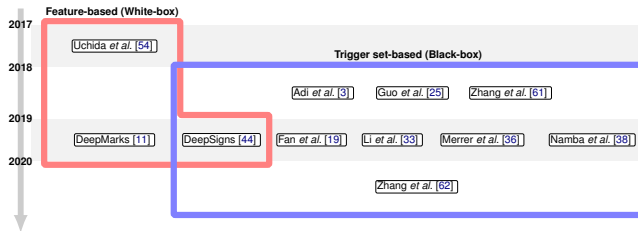


Figure 1: The history of watermark schemes for DNNs.

Figure 1 shows the history of proposed watermark schemes for DNNs. Since Uchida *et al.* [54] proposed the first approach to embedding watermarks into neural networks, various watermarking techniques have been proposed. In terms of their

watermark embedding methodology, these watermarking techniques have been categorized into two types: trigger set-based and feature-based methods. Trigger set-based methods utilize additional training samples for DNNs to remember as watermarks [3, 19, 25, 33, 36, 38, 61, 62]. Feature-based methods embed watermarks by modifying model features [11, 44, 54].

Zhang *et al.* [61] proposed a representative trigger set-based method. They trained a model to learn predefined key pairs, each consisting of a key image and its label, which is different from the original label of the key image. Specifically, they assigned a *false* label with respect to the ground-truth function to the key image. The gist of their approach is that a model without the watermark is highly likely to emit a ground-truth label rather than the predefined false label for a given key image. Therefore, the owner can prove ownership afterwards by querying the model with the key images and checking whether the model outputs the predefined false label. In this scheme, the key images and their predefined false labels become a *trigger set*.

Other trigger set-based watermarking techniques employ more or less similar approaches, but Adi *et al.* [3] further integrated this scheme with cryptographic primitives to secure embedded watermarks. Unlike most researchers who have focused on image classification networks, Zhang *et al.* [62] recently proposed the first watermarking scheme for image processing networks.

2.2 Target Watermark Schemes

Our goal is to evaluate the robustness of state-of-the-art trigger set-based watermark schemes. Thus, we chose 10 representative watermarking algorithms, published at top venues over the past five years [3, 19, 25, 33, 36, 38, 44, 61]. They share a common scheme that uses trigger sets for verifying ownership.

Algorithm 1: Embedding a trigger set into a DNN.

Input : A regular training set (\mathcal{D}_{train}).
A set of source images (I_{src}).
Output : A watermarked model (M_{wm}).
1 **function** EmbedWatermark($\mathcal{D}_{train}, I_{src}$)
2 $I_{key} \leftarrow \text{GenerateKeyImgs}(I_{src})$
3 $L_{target} \leftarrow \text{AssignTargetLabels}(I_{key})$
4 $\mathcal{D}_{trigger} \leftarrow (I_{key}, L_{target})$
5 $M_{wm} \leftarrow \text{TrainModel}(\mathcal{D}_{train}, \mathcal{D}_{trigger})$
6 **return** M_{wm}

Algorithm 1 summarizes how a trigger set-based watermark algorithm embeds the ownership proof of an owner O into a DNN model. O provides a training set \mathcal{D}_{train} and a set of source images I_{src} to the EmbedWatermark function. Given I_{src} , GenerateKeyImgs generates a set of key images I_{key} (Line 2). Note that these key images are intentionally designed to have a different underlying distribution than that of \mathcal{D}_{train} . Owing to the over-parameterization of DNN models, they are capable of intentionally learning key images along

with \mathcal{D}_{train} [16, 60]. The AssignKeyLabels function assigns a target label L_{target} to each key image (Line 3). We call generated key images together with their assigned target labels as a *trigger set* $\mathcal{D}_{trigger}$. Finally, the TrainModel function trains a model with both \mathcal{D}_{train} and $\mathcal{D}_{trigger}$ to embed watermarks (Line 5). This step is analogous to backdoor attacks [12, 24] *per se* but different in that this step is used to claim ownership of a DNN model, instead of emplacing backdoors.

When O claims ownership, they conduct the following verification phase: O queries a model of which the ownership is in doubt with the key images. If the model is indeed the owner’s genuine model, the model will output the predefined target labels trained in the training phase. In Appendix A, we describe each of the 10 selected watermarking algorithms. Throughout the paper, we denote each algorithm as follows: $WM_{content}$ [61], WM_{noise} [61], $WM_{unrelated}$ [61], WM_{mark} [25], $WM_{abstract}$ [3], WM_{adv} [36], $WM_{passport}$ [19], $WM_{encoder}$ [33], WM_{exp} [38], and DeepSigns [44].

3 Adversary Model

We introduce an attack scenario in which an adversary infringes on the IP of a model owner with an exfiltrated DNN model, along with the notations that we use throughout the paper. We then describe the prior knowledge of an adversary regarding the exfiltrated model.

3.1 Attack Scenario

We assume two parties in the attack scenario: a model owner O and an adversary \mathcal{A} . O embeds watermarks into a neural network model M_{org} by training M_{org} with a trigger set, thus producing the watermarked model M_{wm} . O then hosts a service by leveraging M_{wm} . On the other hand, \mathcal{A} decides to steal M_{wm} because training a precise model from scratch requires a lot of computational resources as well as training instances. For instance, \mathcal{A} can steal M_{wm} by compromising O ’s machine learning service server or getting help from an insider. Enumerating the feasible ways of \mathcal{A} obtaining M_{wm} is beyond the scope of this paper.

After stealing M_{wm} , \mathcal{A} hosts a similar service as O using a model M_{adv} derived from M_{wm} . Note that the end goal of \mathcal{A} is to either (1) to obscure O ’s ownership of M_{adv} or (2) to claim ownership of M_{adv} . Therefore, \mathcal{A} may have built M_{adv} by transforming M_{wm} to achieve these goals. That is, M_{wm} and M_{adv} are not necessarily the same. We further elaborate on attack scenarios with these goals in §5.1.

Finally, once O suspects that M_{adv} is derived from M_{wm} , O will attempt to prove their ownership of M_{adv} . However, if O watermarked M_{wm} with a feature-based scheme, O must have white-box access to M_{adv} to verify ownership. Considering that \mathcal{A} certainly wants to hide the true ownership of M_{adv} , \mathcal{A} will not provide white-box access to M_{adv} unless M_{adv} is under litigation. Thus, in this paper, we focus on trigger

Table 1: Summary of adversarial evaluations performed by previous studies.

Attack	$WM_{content}$	WM_{noise}	$WM_{unrelated}$	WM_{mark}	$WM_{abstract}$	WM_{adv}	$WM_{passport}$	$WM_{encoder}$	WM_{exp}	DeepSigns
Fine-tuning	✓	✓	✓	✗	✓	✗	✓	✓	✗	✓
Model Stealing	✗	✗	✗	✗	✗	✗	✗	✗	✗	✗
Parameter Pruning	✓	✓	✓	✗	✗	✓	✓	✗	✓	✓
Evasion	✗	✗	✗	✗	✗	✗	✗	✓	✓	✗
Ownership Piracy	✗	✗	✗	✗	✓	✓	✗	✗	✗	✓
Ambiguity	✓	✓	✓	✗	✗	✗	✓	✗	✗	✗
# of Evaluated Attacks	3	3	3	0	2	2	3	2	2	3

set-based watermark schemes, which only require black-box access for ownership verification.

3.2 Adversarial Knowledge

We assume two adversaries according to their adversarial knowledge: (1) a non-adaptive adversary and (2) an adaptive adversary. A non-adaptive adversary knows that the stolen target model M_{wm} has been watermarked but does not know which specific watermarking algorithm was used. On the other hand, an adaptive adversary knows the exact watermarking algorithm that O harnessed to protect the model among various trigger set-based methods. Specifically, the adaptive adversary only knows the internal working of `GenerateKeyImgs` in Algorithm 1. She does not know the source images (I_{src}) for `GenerateKeyImgs`. She also has no access to the original trigger set ($\mathcal{D}_{trigger}$) as well as the training dataset (\mathcal{D}_{train}).

Note that both adversaries share the same knowledge except about the watermarking algorithm. As both adversaries stole M_{wm} from O , they can observe the model inputs, outputs, and structure. Additionally, we assume that they have access to 50% of a testing set, which is required to launch attacks against M_{wm} . Note that this data accessible by the adversaries is completely disjointed from the original training set, assuming the least privilege granted to them. Previous studies [3, 33, 44, 61] assume similar capabilities for the adversary to conduct different attacks. We further considered adversaries who have access to fewer data in Appendix D.

4 Motivation

We argue that today’s evaluation practice of demonstrating watermark robustness exhibits two common shortcomings: incomplete adversarial evaluation (§4.1) and overlooked adaptive attacks (§4.2).

4.1 Incomplete Adversarial Evaluation

We observe that previous studies on trigger set-based watermarks have evaluated the robustness of their methods using arbitrary choices of the existing attacks, thus demonstrating an upper bound on their robustness only to the selected attacks. Due to the nature of adversarial evaluation, the existence of one effective attack denotes the failure to protect the IP of O , effectively breaking a target watermarking scheme. Therefore, it is paramount to account for all existing attacks to demonstrate meaningful robustness.

Table 1 summarizes the evaluations performed by the previous watermark research in terms of applicable existing attacks. Note from the table that no previous studies evaluated their approaches against a complete set of attacks. Among the six attacks, the researchers only considered at most three attack scenarios and missed other attacks in their evaluations. Moreover, model stealing attacks have never been evaluated in any previous studies.

We emphasize that all six attacks examined herein have existed since each watermarking algorithm was first proposed. In other words, ever since each watermarking algorithm was first proposed, their robustness against several existing state-of-the-art attacks has remained unexplored. Therefore, it is still questionable whether state-of-the-art watermarking algorithms can successfully work as a defense mechanism against various real-world threats.

Furthermore, incomplete adversarial evaluation becomes problematic when comparing the robustness of different watermarking algorithms. Because the previous studies evaluated watermarking algorithms against arbitrarily chosen attacks, they have failed to demonstrate which algorithms are more robust than others in general. Even though one algorithm is robust against a given attack, it can be broken by another attack against which other algorithms are known to be secure. We believe that this incomplete evaluation practice stems from the lack of prior systematic studies that enumerate all the applicable attacks. Thus, in this paper, we summarize these attacks (§5.1).

4.2 Overlooked Adaptive Attacks

A vast volume of recent research on securing machine learning models has striven to demonstrate a meaningful upper bound of its robustness [5, 7, 14, 28, 42, 47]. To this end, they have focused on strong adaptive adversaries who know the adopted defense algorithms for securing the model. Nevertheless, the previous studies on watermarking algorithms have not yet taken into account adaptive attacks in their adversarial evaluation. Therefore, to challenge the robustness of watermarking algorithms to the fullest extent, we propose novel adaptive attacks in the context of DNN watermarking.

Note that the existing attacks in Table 1 are non-adaptive attacks. In addition to these attacks, we consider adaptive

attacks against M_{wm} . The adaptive adversary mounts the same attacks as non-adaptive adversaries. She leverages her prior knowledge of the underlying watermarking algorithm and adapts these attacks, thus mounting strong attacks.

5 Attack Algorithms

We now introduce state-of-the-art attacks that non-adaptive and adaptive adversaries (§3) can conduct. We consolidate six of the existing attacks spread across various studies in the literature and systematically categorize them from the perspective of the goal that the adversaries aim to achieve (§5.1). We then briefly describe each existing attack (§5.2–§5.3). Finally, we present novel attacks that the adaptive adversary is able to conduct via leveraging the knowledge of a target watermarking algorithm (§5.4).

5.1 Attack Overview

An adversary \mathcal{A} can devise two different scenarios to conceal the fact that \mathcal{A} stole M_{wm} from O ; \mathcal{A} can decide to either obscure O 's ownership or claim her ownership.

Obscuring O 's ownership. The goal of \mathcal{A} in this scenario is to thwart O 's ownership verification by modifying M_{wm} , such as by training a counterfeit model or detecting key images. As O fails to verify their ownership in this scenario, \mathcal{A} can successfully obscure O 's ownership and insist that M_{wm} is not watermarked. To achieve this goal, \mathcal{A} can launch fine-tuning, model stealing, evasion, or parameter pruning attacks.

Claiming of ownership by \mathcal{A} . Another scenario that \mathcal{A} can consider is to claim ownership of M_{wm} by implanting a new trigger set into M_{wm} or generating a set of fake key images that can trigger the target labels. Note that \mathcal{A} does not aim to damage O 's ownership and O 's watermark may persist. Therefore, both O and \mathcal{A} can claim ownership based on the respective trigger set, which results in conflicting ownership arguments. Since it is infeasible to decide which one is fraudulently claiming ownership solely based on their key images and target labels, previous studies [3, 19, 36, 44, 61] have considered this to be a plausible strategy. To realize this scenario, \mathcal{A} is able to conduct one of the following two attacks: ownership piracy or ambiguity attacks.

5.2 Obscuring O 's Ownership

Fine-tuning attack. To remove the original watermark, \mathcal{A} can fine-tune M_{wm} with a new training set [3, 13, 19, 33, 44, 61]. Specifically, \mathcal{A} trains M_{wm} with a new small set that shares an underlying distribution with the original training set, thus preventing M_{wm} from losing its original functionality. At the same time, \mathcal{A} does not include any data that are distant from the underlying distribution in the new training set in the expectation that M_{wm} will forget O 's key images.

Model stealing attack. \mathcal{A} in model stealing attacks [39, 53] aims to copy the functionality of M_{wm} into a new model, except for the capability of remembering the trigger set. To this end, \mathcal{A} labels arbitrary images by querying M_{wm} . Using the constructed training set, \mathcal{A} trains a model from scratch. The new model may forget O 's key images because the distribution represented by the arbitrary images is highly likely not to include O 's trigger set.

Parameter pruning attack. As an attempt to make M_{wm} forget a trained trigger set, \mathcal{A} in parameter pruning attack scenarios [19, 36, 38, 44, 61] prunes certain parameters of M_{wm} . The original goal of model pruning is to reduce the number of redundant parameters in DNNs. However, recall that model watermarking is possible due to the over-parameterization of DNNs. \mathcal{A} expects M_{wm} to lose the capability of remembering the key images after the pruning of some trained parameters, thus causing O 's ownership claim to fail.

Evasion attack. \mathcal{A} conducting evasion attacks [33, 35, 38] may attempt to detect key images on the fly when O queries M_{wm} . Recall that key images do not belong to the underlying distribution of regular images. Thus, \mathcal{A} can distinguish key images by checking the distribution of a given image. Once \mathcal{A} finds a suspicious image, she can evade the verification process by returning a random label.

5.3 Claiming of Ownership by \mathcal{A}

Ownership piracy attack. In ownership piracy attacks [3, 36, 44], \mathcal{A} attempts to implant her own new trigger set into M_{wm} to claim ownership. Specifically, \mathcal{A} prepares a new trigger set that is different from the original and then retrains M_{wm} with the new trigger set. After training, M_{adv} will classify \mathcal{A} 's key images as their target labels, and \mathcal{A} can fraudulently claim ownership with M_{adv} , which leads to conflicting ownership arguments.

Ambiguity attack. To claim ownership, in an ambiguity attack scenario [19, 21, 61], \mathcal{A} generates a set of counterfeit key images that can trigger the target labels. Similar to model inversion attacks [21], \mathcal{A} gradually updates regular images by leveraging gradient descent so that M_{wm} classifies the updated images as their predefined labels. The core difference of this attack compared to ownership piracy attacks is that the adversary in this scenario does not modify M_{wm} but creates counterfeit key images by leveraging M_{wm} .

Assume a scenario where \mathcal{A} launches an ambiguity attack against M_{wm} trained on CIFAR-10 and watermarked using $WM_{content}$. \mathcal{A} can add quasi-imperceptible perturbations to “apple” images taken from CIFAR-100 such that M_{wm} classifies each image as an “airplane.” In this scenario, \mathcal{A} can verify ownership based on $WM_{unrelated}$ using the perturbed images as key images.

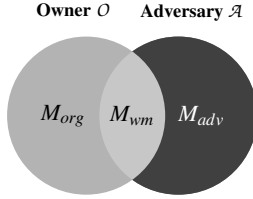


Figure 2: The difference between models accessible to A who aims to claim her ownership and O .

5.3.1 Shortcomings of Evaluation

Recall from §5.1 that ownership piracy and ambiguity attacks inevitably cause a stalemate between A and O with conflicting ownership arguments based on their respective watermarks. In this regard, previous studies [3, 19, 36, 44, 61] have demonstrated the degree to which their watermarking algorithms can withstand these attacks. However, we claim that there exists a straightforward solution to manifest the true owner in these attack scenarios; thus, their evaluation should have been performed assuming a different scenario.

We note that there exists a clear difference between the capabilities of O and A , as shown in Figure 2. Because A steals the model after O watermarks M_{org} , A cannot access M_{org} which does not have any watermarks. Accordingly, in court, a judge may request that both O and A provide a functional model without any watermarks. Then, O can prove ownership by providing M_{org} , which A cannot provide. A will lose this ownership dispute game due to the inability to present a functional model that remembers none of the key images.

We emphasize that A in ownership piracy or ambiguity attack scenarios does not possess the aforementioned functional model without key images. One may argue that A can present this model to the court by conducting an attack that removes O 's watermark. In this case, A will not conduct ownership piracy or ambiguity attacks because removing watermarks from M_{wm} is enough to infringe the IP of O .

This verification leveraging the adversary's inability of presenting a watermark-free model is analogous to that in traditional image and video watermarking research [2, 17]. To prevent the threat of an adversary claiming ownership by means of blending her watermarks on top of the owner's watermarked image, it is common in the verification to ask the adversary to present the original image without any watermarks.

Therefore, we propose the following more plausible scenario in which A can successfully claim her ownership. In order to claim A 's ownership, we insist that A should first mount an attack that removes O 's watermark and then launch attacks devised to claim A 's ownership against the watermark-removed model, thus constructing a model that only remembers A 's trigger set. Unfortunately, no previous studies have considered these attacks together. On the contrary, we considered this new scenario by performing ownership piracy and

ambiguity attacks against target models after removing O 's watermark (§7.4).

5.4 Adaptive Attacks

We argue that the robustness of watermarked models should not be undermined by the adversary's prior knowledge of target watermarking algorithms. Considering that any insiders are able to leak the algorithms, solely depending on the security by obscurity is not a desirable goal that follow-up watermarking studies pursue. Carlini *et al.* have also emphasized the necessity of evaluations against adaptive attacks for demonstrating adversarial robustness [6].

To this end, we propose novel adaptive attacks in which the adversary can adapt their attacks to a given watermarking scheme. In adaptive attacks, the adversary aims to obscure O 's ownership by modifying M_{wm} to remove O 's trigger set. For this, the adaptive adversary removes O 's trigger set by employing the same fine-tuning, model stealing, and pruning attacks (§5.2). The key difference is that this adversary engineers a new trigger set that plays a role similar to O 's trigger set against M_{wm} and leverages this new trigger set when launching the aforementioned three watermark removal attacks. In the following, we explain how the adversary can adaptively create the new trigger set based on M_{wm} 's watermarking algorithm.

We propose a general framework that the adaptive adversary leverages to create a new trigger set. Since the adversary seeks to generate new key images that serve as O 's key images, the new key images should have an underlying distribution similar to that of the original key images. At the same time, the new key images should be able to trigger attacker-specified target labels. To achieve these two goals, we propose to train an autoencoder such that (1) the output images have a distribution similar to images that the watermarking scheme of M_{wm} generates and (2) M_{wm} classifies each output image as a target label. Note that the adaptive adversary can train such an autoencoder by leveraging her knowledge about the target watermarking scheme and white-box access to the stolen target model. Specifically, given a source image x and a target label y_t , the adversary trains the autoencoder to minimize the following loss function.

$$\begin{aligned} x' &= \text{AutoEncoder}(x) \\ L(x, y_t) &= L_{ae}(x, x') + \lambda \cdot L_f(y_t, f(x')) \end{aligned} \quad (1)$$

In Equation 1, the loss function has two terms: L_{ae} and L_f . These terms are designed to achieve the autoencoder's two training objectives, respectively. L_{ae} refers to a relationship between the input and output images that the adversary can adaptively define based on a target watermarking scheme, and L_f refers to the classification error of a target model.

To perform strong attacks, it is important to choose well-suited source images x and a loss function L_{ae} so that the autoencoder is able to learn how a target watermarking scheme

performs the `GenerateKeyImgs` function in Algorithm 1 with high fidelity. For instance, consider $WM_{abstract}$ [3] as a target watermarking scheme. In this case, the adversary can use arbitrary abstract images collected from the Internet as source images and choose the mean squared error loss function as L_{ae} so that the output images x' become abstract images that can trigger target labels when given to M_{wm} . We describe the source images and loss functions that we chose to model each of our target watermarking schemes in Appendix B. Note that we have devised fine-tuning, model stealing, and parameter pruning adaptive attacks for each watermarking scheme, yielding 30 attack variants (3 attacks \times 10 schemes).

Besides the source images x and the loss function L_{ae} , the adaptive adversary also needs to specify the target label y_t to train this autoencoder but has no prior knowledge about the target labels of the original key images. Therefore, the adversary repeatedly trains this autoencoder for each class while assuming the current class as a target label. Then, the adversary collects trigger set pairs (x', y_t) from all trained autoencoders and leverages all the collected pairs when initiating the watermark removal attacks. The adversary expects these trigger set pairs to effectively contribute to removing the original trigger set of a target model.

6 Implementation

We implemented the target watermarking algorithms and attacks in Python 3.6.9. In particular, we used Keras 2.3.1 [15] on top of TensorFlow 2.1.0 [1] for training DNN models, embedding watermarks, and the attacks. However, we implemented the attacks targeting $WM_{passport}$ in PyTorch 1.4.0 [51] as $WM_{passport}$, which was originally implemented in PyTorch, requires a huge engineering effort to migrate to Keras. The remaining nine target algorithms were implemented by referring to their papers and code if available.

7 Evaluation

In this section, we evaluate the robustness of the 10 trigger set-based watermarks. We first explain the datasets and DNN models that we used (§7.1) and demonstrate how we successfully implanted watermarks into the DNN models using the target watermark schemes in our experimental settings (§7.2). We then conduct the adversarial evaluation of each attack that we have discussed so far (§7.3.1–§7.4.2).

7.1 Datasets and Target Models

Dataset. We use the MNIST, GTSRB, CIFAR-10, and CIFAR-100 datasets. All the prior studies have only evaluated their algorithms using at most three datasets except WM_{exp} [38], which used four. To keep aligned with the research that used the most datasets, we use these four widely adopted datasets.

Table 2: Performance of the target models M_{wm} on four datasets: MNIST (MN), GTSRB (GT), CIFAR-10 (C10), and CIFAR-100 (C100). Numbers in parentheses denote the degree to which test accuracy dropped compared to a model without watermarks.

	Trigger Set Recall (%)				Test Acc. (%)			
	MN	GT	C10	C100	MN	GT	C10	C100
$WM_{content}$	99.90	100	100	100	98.85 (-0.21)	94.75 (-0.28)	93.09 (0.12)	71.71 (-0.66)
WM_{noise}	100	100	100	100	99.04 (-0.02)	94.89 (-0.13)	93.20 (0.23)	72.77 (0.40)
$WM_{unrelated}$	99.94	100	100	100	99.02 (-0.04)	94.32 (-0.70)	92.91 (-0.06)	72.51 (0.14)
WM_{mark}	98.72	99.72	99.64	94.79	98.94 (-0.12)	96.56 (1.53)	92.42 (-0.55)	70.85 (-1.52)
$WM_{abstract}$	100	100	100	100	99.02 (-0.04)	95.08 (0.06)	92.93 (-0.04)	72.46 (0.09)
WM_{adv}	100	100	100	100	99.21 (0.15)	97.21 (2.18)	91.79 (-1.18)	71.78 (-0.59)
$WM_{passport}$	84.00	100	82.00	93.00	99.12 (-0.23)	94.29 (0.95)	88.63 (-2.72)	63.17 (-4.87)
$WM_{encoder}$	100	96.94	99.20	99.20	98.98 (-0.08)	93.13 (-1.90)	92.67 (-0.30)	72.19 (-0.18)
WM_{exp}	100	100	100	100	99.07 (0.01)	94.54 (-0.49)	92.62 (-0.35)	71.53 (-0.84)
DeepSigns	100	100	100	100	99.09 (0.03)	95.79 (0.76)	91.69 (-1.28)	70.27 (-2.10)

DNN models. For MNIST, we prepared LeNet-5 models [32]. For the remaining datasets, we implemented ResNet-56 models [26]. However, we employed ResNet-18 for all four datasets to evaluate $WM_{passport}$ in the same setup as provided by the authors (recall §6). Note that these models have been widely adopted in previous studies [3, 19, 25, 33, 38]. Both the LeNet and ResNet models show outstanding performance; therefore, they are highly likely to be deployed in real-world cases, rendering them good target models for watermark implantation.

7.2 Embedding Watermarks into the DNN Models

To build M_{wm} , we watermarked the DNN models trained on the four datasets by leveraging each algorithm, yielding a total of 40 target DNN models (4 datasets \times 10 schemes). Note that each M_{wm} should maintain its classification accuracy and emit the predefined target labels for given key images.

Table 2 shows the recall rate of watermark key images and accuracy for the test instances on M_{wm} . The second to the fifth columns summarize the trigger set recall of M_{wm} across datasets, the fraction of the watermark key images that are correctly classified as their target labels. Most M_{wm} correctly remember their trigger sets and classify key samples with a high recall of over 99%. The sixth to the ninth columns describe the test accuracy for M_{wm} as well as the magnitude of drops in test accuracy in comparison to the corresponding

Table 3: Trigger set recall (%) of M_{adv} after fine-tuning attacks.

	Non-adaptive Attack				Adaptive Attack			
	MN	GT	C10	C100	MN	GT	C10	C100
$WM_{content}$	57.02	0.36	24.54	13.20	39.74	53.96	26.92	75.20
WM_{noise}	5.93	84.46	99.14	93.80	0.36	5.63	3.78	10.20
$WM_{unrelated}$	99.34	100	99.10	92.80	32.76	99.77	17.26	0.00
WM_{mark}	40.28	8.95	3.86	2.29	19.77	25.87	8.02	1.46
$WM_{abstract}$	51.00	51.00	60.00	26.00	45.00	83.00	54.00	23.00
WM_{adv}	35.00	79.00	24.00	13.00	14.00	8.00	12.00	2.00
$WM_{passport}$	14.00	43.00	14.00	3.00	13.00	43.00	17.00	3.00
$WM_{encoder}$	20.00	4.08	20.00	8.00	17.00	7.14	20.60	5.60
WM_{exp}	6.00	0.00	1.00	1.00	7.00	0.00	2.00	0.00
DeepSigns	11.00	1.00	8.00	0.00	11.00	1.00	12.00	2.00

models without any watermark. We observe that most M_{wm} preserve their classification performance after watermarking, showing only a slight drop of within 2%.

However, the models watermarked using $WM_{passport}$ yielded relatively low trigger set recall levels and experienced the largest drops in test accuracy compared to the other target models. Note that this scheme utilizes abstract images as its key images. We used the original $WM_{passport}$ implementation, resulting in no differences between our implementation and that of the authors; we believe that this result stems from using a different set of abstract key images.

Based on the experimental results, we confirm that each M_{wm} yields high test accuracy and high watermark recall. In the remaining sections, we evaluate the presented attacks using these watermarked models.

7.3 Obscuring O 's Ownership

An adversary seeking to obscure O 's ownership attempts to thwart O 's ownership verification process. For this, the adversary can employ fine-tuning, model stealing, evasion, or parameter pruning attacks against M_{wm} , thus generating M_{adv} with a low O 's trigger set recall. At the same time, the test accuracy of M_{adv} should not drop significantly as the adversary needs to host a functional service by leveraging M_{adv} . We now evaluate each attack in this category assuming both non-adaptive and adaptive adversaries.

7.3.1 Fine-tuning Attack

Non-adaptive attack. A non-adaptive adversary tunes M_{wm} on a dataset that does not include any key images, thus constructing another model M_{adv} . Similar to the method proposed by Chen *et al.* [13], we collected arbitrary images for fine-tuning M_{wm} . We then labeled each collected image with the output of M_{wm} . For M_{wm} trained on MNIST, we collected all images from the Fashion-MNIST dataset [57]. We took images from CIFAR-100 for fine-tuning the GTSRB models. For M_{wm} trained on CIFAR-10 and CIFAR-100, we collected

images from each other's dataset. As \mathcal{A} has access to 50% of a test set, we also leveraged this dataset to fine-tune M_{wm} .

Adaptive attack. In addition to these training instances, the adaptive adversary harnesses the autoencoder-generated key images to make M_{wm} unlearn O 's trigger set. Recall from §5.4 that this adversary collects x' , which is designed to resemble O 's key images that trigger y_i . Therefore, the adversary assigns a random label other than y_i to x' and provides this pair as a training instance for fine-tuning attacks, expecting that M_{adv} will interpret O 's key images as the adversary-chosen random classes.

When fine-tuning M_{wm} , we optimized M_{wm} using Adam [30] and trained M_{wm} for 10 epochs. We fixed the learning rates at 0.01 and 0.0005 for MNIST and the other datasets, respectively, except for one case: for M_{wm} trained on the CIFAR datasets and watermarked using $WM_{passport}$, we used a fixed learning rate of 0.0001. We selected these learning rates after exploratory experiments.

Table 3 presents the trigger set recall of M_{adv} , which is the resulting model after conducting fine-tuning attacks on M_{wm} . Note that it is challenging to set a minimum trigger set recall sufficient to prove O 's ownership. Thus, in the table, we colored the cells of vulnerable watermarking schemes that rendered a trigger set recall lower than the threshold varying from 10% to 80%. The gradations represent the extent to which the model is vulnerable to the attacks. We excluded M_{adv} that exhibited over a 5% drop in test accuracy because these models do not suffice for the adversary's goal of hosting functional services. In Appendix E, we include an expanded version of Table 3 that displays the test accuracies of M_{adv} as well as their trigger set recalls.

The left half of the table shows the results for the non-adaptive attacks. When we set 10% as the minimum trigger set recall to prove ownership, the non-adaptive fine-tuning attacks only worked against the 12 target models. However, the number of vulnerable target models jumped to 26 in total when the minimum requirement was set to 80%. Interestingly, all models watermarked using WM_{mark} and DeepSigns were vulnerable to this fine-tuning attack. On the other hand, all models watermarked with $WM_{unrelated}$ were robust, demonstrating trigger set recalls of over 92% for all the datasets.

The right half of the table summarizes the results for the adaptive attacks. Note in the table that the adaptive attacks further destroyed schemes that were robust to the non-adaptive attacks. For instance, WM_{noise} and $WM_{unrelated}$ models exhibited significant trigger set recall drops. On the other hand, the GTSRB model with $WM_{unrelated}$ was still robust to the adaptive attack. This is because the collected arbitrary images from CIFAR-100 with their output labels, which are used for fine-tuning $WM_{unrelated}$, help to resist unlearning O 's trigger set. Note that the primary goal of these CIFAR-100 images is to preserve the test accuracy of $WM_{unrelated}$ after conducting the fine-tuning attack. In case of GTSRB, 10% of its test data was enough to preserve the test accuracy. There-

fore, we removed the arbitrary images from CIFAR-100 when fine-tuning $WM_{unrelated}$, and O 's trigger set recall then decreased to 0%. Considering that the adversary can take either approach, we conclude that $WM_{unrelated}$ is vulnerable to the adaptive fine-tuning attack.

We emphasize that none of the previous studies conducted the adaptive attack even though they are mostly vulnerable to this attack. Furthermore, although seven out of the 10 watermarking algorithms had already been evaluated against fine-tuning attacks in previous studies [3, 19, 33, 44, 61], our analysis reveals that many of them are still vulnerable. This implies that fine-tuning attacks that previous studies have conducted were too weak to construct a meaningful upper bound of their watermarking algorithms. Therefore, we recommend that follow-up studies evaluate their schemes against fine-tuning attacks with sufficiently strong settings and demonstrate the extent to which their watermarks can withstand attacks without being removed. We further investigate various attack settings that can affect the strength of fine-tuning attacks in Appendix C.

7.3.2 Model Stealing Attack

In model stealing attacks, an adversary does not have enough training instances to train a new model from scratch. Thus, the adversary prepares a set of arbitrary images and leverages M_{wm} to label these images. The adversary then trains M_{adv} from scratch on these instances, thereby copying M_{wm} 's functionality except for the capability of remembering the trigger set. We consider both non-adaptive and adaptive adversaries in evaluating the target models against model stealing attacks. **Non-adaptive attack.** To collect training instances, we took the same approach as we did for fine-tuning attacks (§7.3.1). For training, we selected M_{adv} to have the same model structure as M_{wm} . Note that the adversary knows the exact structure of M_{wm} because M_{wm} is already in her hands. We performed model stealing attacks by training this new model from scratch with the collected dataset.

Adaptive attack. The adaptive adversary in this attack scenario also leverages the trigger set created with the autoencoders to preclude M_{adv} from learning O 's trigger set. The adversary prepares training instances in the exact same way as the adaptive adversary in fine-tuning attacks and appends them to the training set for training M_{adv} . Because the adversary feeds x' with a random label to M_{adv} for its training, this new model cannot learn O 's trigger set.

Table 4 summarizes the experimental results of model stealing attacks. We shaded (in red) the cells according to the same criteria as we did for Table 3. The left half of the table presents the results from the non-adaptive attacks. Overall, the target models underwent a more drastic trigger set recall drop compared to fine-tuning attacks. Assuming the minimal trigger set recall to be 10%, 16 target models were vulnerable to this attack. When we consider 80% as the minimal requirement,

Table 4: Trigger set recall (%) of M_{adv} after model stealing attacks.

	Non-adaptive Attack				Adaptive Attack			
	MN	GT	C10	C100	MN	GT	C10	C100
$WM_{content}$	82.94	0.00	2.04	0.80	28.37	0.05	1.18	0.40
WM_{noise}	0.21	59.19	3.60	45.60	0.09	6.76	4.04	87.60
$WM_{unrelated}$	99.76	100	95.26	0.00	34.94	100	9.02	0.00
WM_{mark}	11.57	5.10	2.32	0.90	7.66	7.27	6.81	1.46
$WM_{abstract}$	41.00	35.00	24.00	2.00	39.00	48.00	27.00	2.00
WM_{adv}	23.00	70.00	8.00	11.00	17.00	0.00	16.00	1.00
$WM_{passport}$	7.00	34.00	19.00	2.00	7.00	37.00	16.00	1.00
$WM_{encoder}$	9.67	2.55	12.60	1.80	9.33	2.30	13.20	1.40
WM_{exp}	1.00	0.00	2.00	0.00	4.00	0.00	2.00	2.00
DeepSigns	10.00	3.00	6.00	1.00	6.00	2.00	11.00	0.00

Table 5: Trigger set recall (%) of M_{adv} after parameter pruning attacks.

	Non-adaptive Attack				Adaptive Attack			
	MN	GT	C10	C100	MN	GT	C10	C100
$WM_{content}$	99.87	100	100	100	64.95	100	100	100
WM_{noise}	100	100	100	100	97.29	0.27	100	58.20
$WM_{unrelated}$	99.38	100	100	100	17.22	0.81	90.98	4.00
WM_{mark}	97.40	99.64	99.64	94.63	69.03	97.03	96.97	69.96
$WM_{abstract}$	73.00	100	100	100	78.00	95.00	97.00	98.00
WM_{adv}	91.00	100	100	100	96.00	7.00	97.00	94.00
$WM_{passport}$	80.00	100	71.00	87.00	84.00	94.00	82.00	91.00
$WM_{encoder}$	96.50	96.94	99.20	98.60	99.00	91.07	98.20	92.80
WM_{exp}	92.00	100	100	100	92.00	99.00	98.00	97.00
DeepSigns	39.00	89.00	100	98.00	81.00	98.00	99.00	78.00

25 models failed to verify O 's ownership. Among the 10 watermarking schemes, M_{wm} with WM_{exp} and DeepSigns were the most vulnerable models, showing a trigger set recall of below 10% after the attacks.

The right half of the table shows the results of the adaptive model stealing attacks. Considering 10% as the required minimal trigger set recall, the watermarks embedded in 18 out of the 40 target models were destroyed by the adaptive attack. We also note that the trigger set recalls further decreased in most target models compared to the non-adaptive attack. Moreover, when we raise the bar to 80%, all 10 watermarking schemes were broken by this attack. Although $WM_{unrelated}$ was robust against the non-adaptive model stealing attack, it was destroyed by the adaptive attack.

Note that most target models were vulnerable to the non-adaptive and adaptive model stealing attacks. This means that the current watermark evaluation practice does not consider the real-world threats properly. We stress that researchers should evaluate robustness against the complete set of attacks, including model stealing attacks, and raise the bar of watermarking schemes' robustness with aggressive evaluation that considers an adaptive adversary.

7.3.3 Parameter Pruning Attack

The non-adaptive and adaptive adversaries in parameter pruning attacks attempt to prune the parameters of M_{wm} .

Non-adaptive attack. To erase O 's watermark, the non-adaptive adversary prunes $p\%$ of the smallest parameters in M_{wm} , thus building a new model M_{adv} .

Adaptive attack. In adaptive pruning attacks, the adversary identifies parameters that contribute to the classification of O 's trigger set by leveraging the autoencoder-generated trigger set and then removes those parameters. Specifically, the adversary observes the differences between the neuron activations of M_{wm} when x and x' are given. Note that the neurons that render different behaviors between these images can be regarded as trigger set-related. The adversary thus prunes $p\%$ of parameters that showed the greatest differences. After pruning, M_{adv} becomes non-reactive to O 's trigger set. When pruning parameters, we only considered parameters that belong to the fully connected layers.

Table 5 presents the trigger set recall of M_{adv} after parameter pruning attacks. We evaluated the effect of this attack with six different values of p : 5, 10, 20, 40, 60, and 80. Among the results for the six different p values, we only show the results that reported the lowest trigger set recall with a test accuracy drop of less than 5%. We colored the cells according to the same criteria that we set for Table 3. The left half shows the trigger set recall after the non-adaptive attacks. In general, we found that the watermarking schemes are robust against this attack, which accords with the experimental results of previous studies [19, 36, 38, 44, 61]. Four out of 30 target models showed a trigger set recall of less than 80%; only one model was weak against this attack when we considered 40% as the minimal recall required to prove ownership.

The right half of the table summarizes the experimental results after the adaptive pruning attacks. The adaptive pruning attacks were not as strong as other adaptive attacks; however, the adaptive attack damaged four target models that were robust to the non-adaptive attacks. Furthermore, note that the $WM_{unrelated}$ models tend to demonstrate a significant drop in the trigger set recall, although they experience non-trivial test accuracy drops as well (see Table 14). These results suggest the necessity of our adaptive pruning attacks against the existing watermarking algorithms.

7.3.4 Evasion Attack

The goal of \mathcal{A} in performing an evasion attack is to distinguish queries that have key images from normal queries. Once a key image is identified, the adversary may return random labels to drop the trigger set recall, thus obscuring O 's ownership.

To assess \mathcal{A} 's capability of distinguishing key images from regular images, we trained autoencoders for each class of images with 50% of a test set. For instance, we prepared a total of 100 autoencoders for CIFAR-100. We then evaluated

Table 6: Trigger set detection accuracies when performing evasion attacks against the target models. A table cell in the red background represents a vulnerable model that enables \mathcal{A} to achieve an accuracy for detecting the trigger set of over 85%, and the gradations represent the extent to which the model is vulnerable to evasion attacks.

	Detection Acc. (%)			
	MNIST	GTSRB	CIFAR-10	CIFAR-100
$WM_{content}$	98.31	97.57	98.62	89.20
WM_{noise}	98.38	97.75	99.64	90.30
$WM_{unrelated}$	98.32	97.91	49.73	86.70
WM_{mark}	98.29	93.18	93.88	86.38
$WM_{abstract}$	99.50	87.00	67.50	81.00
WM_{adv}	99.50	97.50	100	91.00
$WM_{passport}$	99.50	89.00	60.50	78.50
$WM_{encoder}$	94.75	85.59	89.40	87.10
WM_{exp}	62.50	85.50	78.00	82.00
DeepSigns	100	97.00	100	93.00

whether the trained autoencoders could output an image similar to the input image. Note that these autoencoders are able to reconstruct normal images well but fail with key images as the autoencoders are trained on regular images. To decide whether the autoencoders fail to reconstruct given images, we computed three metrics, i.e., L_1 norms, L_2 norms, and Jensen-Shannon divergence, between the input and output images as in the approach of [35].

Specifically, given an image, we query M_{wm} and record the output class. We then reconstruct the image with the autoencoder of the output class and compute the metrics. If all three metrics computed from the image are lower than the thresholds, we consider the given image to be a normal one. We set the thresholds such that false-positive rates are at most 0.1% on the set of images used for training the autoencoders.

Table 6 summarizes the detection accuracies of evasion attacks. We balanced the number of key images and regular images when measuring the detection accuracy so that the baseline detection accuracy is 50%. These regular images were taken from the training set so that they would not overlap with the images used to train the autoencoders. A high detection accuracy implies that the adversary can successfully reduce the trigger set recall without losing test accuracy.

Note in the table that 32 target models out of 40 can successfully evade the verification process as they reported at least 85% detection accuracies. This is not surprising as only two out of the 10 previous studies have considered evasion attacks in their adversarial evaluation. Among the two previous studies that considered evasion attacks, WM_{exp} is robust against this attack, as shown in the table. This is because it takes key images from exactly the same distribution as the regular images used for training WM_{exp} . However, $WM_{encoder}$ was vulnerable to evasion attacks in our settings, even though a previous study [33] demonstrated its robustness against this attack scenario. That is, the previous study took a naive ap-

proach to conducting evasion attacks so that it failed to demonstrate a meaningful upper bound on its robustness against evasion attacks (see Appendix C).

7.4 Claiming of Ownership by \mathcal{A}

The goal of a non-adaptive adversary claiming her ownership is to cause a stalemate in the ownership dispute game against O . To simulate this adversary, all prior research has considered a scenario where an adversary conducts single ownership piracy or ambiguity attacks. However, there exists an obvious solution to identify the authentic owner; thus the adversary necessarily loses in this game (§5.3.1).

With this in mind, we propose a new attack scenario that incorporates watermark removal attacks within ownership claiming attacks. Specifically, we consider a novel scenario where the adversary first removes O 's watermark and then implants \mathcal{A} 's watermark, thus claiming ownership of a new model that only holds \mathcal{A} 's watermark. Among the watermark removal attacks, we chose models constructed via model stealing attacks as a base for ownership piracy and ambiguity attacks due to model stealing attacks' outstanding performance in removing watermarks (recall §7.3.2).

Recall that the non-adaptive adversary in these attack scenarios claims ownership based on her own trigger set. In other words, the adversary needs to choose one watermarking algorithm to prepare her trigger set. For this, we assumed that \mathcal{A} prepares her trigger set using $WM_{unrelated}$. Hence, $WM_{unrelated}$ becomes the basis of \mathcal{A} 's fraudulent ownership claim of the resulting model M_{adv} .

7.4.1 Ownership Piracy Attack

To perform piracy attacks, the adversary follows the same procedures and settings as fine-tuning attacks. The only difference is that \mathcal{A} also appends her trigger set to the dataset of a fine-tuning attacker. With this dataset, \mathcal{A} fine-tunes a watermark-removed model to embed her trigger set.

Table 7 presents the trigger set recalls of \mathcal{A} and O after the attack. We compare these two trigger set recalls because \mathcal{A} in this attack insists that M_{adv} only contains \mathcal{A} 's trigger set and has never been trained on O 's trigger set. That is, \mathcal{A} aims to demonstrate that \mathcal{A} 's trigger set recall is high, whereas O 's trigger set recall is low. We thus show the differences between the trigger set recall rates of \mathcal{A} and O in parentheses. We shaded (in red) the target models that showed a difference greater than a threshold varying from 20% to 80%. The gradations illustrate the magnitude of each trigger recall difference. As we did for all other attacks, we excluded target models with a test accuracy drop of over 5%.

Since we removed O 's watermark before embedding \mathcal{A} 's watermark, \mathcal{A} 's trigger set acquired a dominant position over that of O from 22 target models. Furthermore, from 19 target models, \mathcal{A} 's trigger set recall surpassed O 's by at least 60%.

Table 7: Trigger set recalls of M_{adv} after ownership piracy attacks. Numbers in parentheses denote the differences of trigger set recalls between \mathcal{A} and O .

	\mathcal{A} 's Trigger Set Recall (%)				O 's Trigger Set Recall (%)			
	MN	GT	C10	C100	MN	GT	C10	C100
$WM_{content}$	86.00 (36.24)	99.00 (98.96)	100 (99.72)	100 (99.80)	49.76	0.05	0.28	0.20
WM_{noise}	92.00 (91.91)	99.00 (74.95)	100 (97.20)	100 (78.00)	0.09	24.05	2.80	22.00
$WM_{unrelated}$	96.00 (86.72)	98.00 (37.28)	94.00 (43.48)	99.00 (99.00)	9.28	60.72	50.52	0.00
WM_{mark}	87.00 (75.46)	99.00 (93.38)	98.00 (94.94)	100 (99.32)	11.54	5.62	3.06	0.68
$WM_{abstract}$	89.00 (61.00)	99.00 (67.00)	98.00 (81.00)	100 (100)	28.00	32.00	17.00	0.00
WM_{adv}	75.00 (41.00)	91.00 (79.00)	98.00 (92.00)	100 (93.00)	34.00	12.00	6.00	7.00
$WM_{passport}$	94.00 (89.00)	0.00 (-6.00)	0.00 (-10.00)	15.00 (14.00)	5.00	6.00	10.00	1.00
$WM_{encoder}$	98.00 (88.00)	100 (97.70)	100 (88.20)	100 (99.00)	10.00	2.30	11.80	1.00
WM_{exp}	70.00 (70.00)	98.00 (98.00)	98.00 (96.00)	100 (100)	0.00	0.00	2.00	0.00
DeepSigns	93.00 (88.00)	100 (98.00)	99.00 (92.00)	100 (100)	5.00	2.00	7.00	0.00

These results imply that \mathcal{A} can successfully take ownership of those target models, claiming that those models only contain \mathcal{A} 's trigger set. Considering these results, we suggest future researchers prove their algorithms' robustness against piracy attacks based on our new scenario.

7.4.2 Ambiguity Attack

Unlike the previous adversary, an adversary performing ambiguity attacks does not implant \mathcal{A} 's trigger set into the watermark-removed model. Instead, \mathcal{A} generates key images that can trigger the adversary-chosen target labels when given to the watermark-removed model. Consequently, \mathcal{A} can claim that the resulting model only remembers \mathcal{A} 's trigger set. Specifically, \mathcal{A} perturbs seed images by leveraging gradient descent in order to divert the classification of the perturbed images towards the adversary-chosen target label [21].

Table 8 summarizes the ambiguity attack results. We applied the same criteria as piracy attacks to color each cell. Since \mathcal{A} does not modify the watermark-removed model, O 's trigger set recalls after this attack are same as those shown in Table 4. Among 40 target models, \mathcal{A} 's trigger set recalls from 23 target models were greater than O 's by at least 20%. We note that the L_2 norm of perturbations added to the seed images is less than 0.004 on average, which implies that the added perturbations are quasi-imperceptible. We thus conclude that \mathcal{A} can successfully claim her ownership of those models with the created trigger set. As we demonstrated the effectiveness of this attack, we argue that future research should also evaluate its algorithm against ambiguity attacks.

Table 8: Trigger set recalls of M_{wm} after ambiguity attacks. Numbers in parentheses denote the differences of trigger set recalls between \mathcal{A} and \mathcal{O} .

	\mathcal{A} 's Trigger Set Recall (%)				\mathcal{O} 's Trigger Set Recall (%)			
	MN	GT	C10	C100	MN	GT	C10	C100
$WM_{content}$	100 (17.06)	98.00 (98.00)	100 (97.96)	100 (99.20)	82.94	0.00	2.04	0.80
WM_{noise}	100 (99.79)	98.00 (38.81)	100 (96.40)	100 (54.40)	0.21	59.19	3.60	45.60
$WM_{unrelated}$	98.00 (-1.76)	100 (0.00)	100 (4.74)	97.00 (97.00)	99.76	100	95.26	0.00
WM_{mark}	100 (88.43)	100 (94.90)	100 (97.68)	94.00 (93.10)	11.57	5.10	2.32	0.90
$WM_{abstract}$	100 (59.00)	100 (65.00)	100 (76.00)	100 (98.00)	41.00	35.00	24.00	2.00
WM_{adv}	100 (77.00)	100 (30.00)	100 (92.00)	100 (89.00)	23.00	70.00	8.00	11.00
$WM_{passport}$	100 (93.00)	48.00 (14.00)	0.00 (-19.00)	41.00 (39.00)	7.00	34.00	19.00	2.00
$WM_{encoder}$	100 (90.33)	99.00 (96.45)	100 (87.40)	100 (98.20)	9.67	2.55	12.60	1.80
WM_{exp}	48.00 (47.00)	0.00 (0.00)	100 (98.00)	0.00 (0.00)	1.00	0.00	2.00	0.00
DeepSigns	100 (90.00)	100 (97.00)	100 (94.00)	98.00 (97.00)	10.00	3.00	6.00	1.00

8 Lessons

We have so far conducted six different attacks along with three adaptive attacks to evaluate the robustness of the 10 watermarking algorithms. Table 9 shows the number of attacks that succeeded in each target model watermarked using the given algorithm. When tallying up the totals, we only included results that reported a test accuracy drop of at most 5%. We set a trigger set recall of 80% as the minimum threshold for claiming ownership after conducting fine-tuning, model stealing, and parameter pruning attacks. For evasion attacks, we considered 85% as the minimal detection accuracy necessary to evade the verification step.

Note in the table that every watermarking algorithm is broken by at least two presented adaptive attacks and two non-adaptive attacks. When considering both adaptive and non-adaptive attacks, all schemes do not demonstrate the robustness against at least five attacks. Furthermore, five out of the 10 watermarking algorithms [3, 19, 33, 44, 61] were vulnerable to attacks against that the authors had already evaluated. While all the evaluated watermarking algorithms were broken, $WM_{unrelated}$ was the most robust algorithm among them.

These results highlight that all the existing trigger set-based watermarking algorithms are not ready for real-world deployment. We believe that the demonstrated failure to establish the robustness stems from current research practice regarding how adversarial evaluation is conducted. We further discuss several factors that make robust watermarks (§8.1) and suggestions for adversarial evaluation (§8.2).

8.1 Robustness of Watermarking Algorithms

We analyze what makes a particular watermarking algorithm more resilient to adversarial attacks than the others.

Effect of target labels. As shown in Table 9, WM_{noise} and $WM_{unrelated}$ are more robust than the other algorithms against non-adaptive fine-tuning attacks. Note that the key difference between these two schemes and the others is that they allocate a single class to all key images, whereas the remaining schemes assign different labels to each key image. That is, the consistent labeling of these two schemes helps M_{wm} generalize on \mathcal{O} 's trigger set, thus making it difficult for \mathcal{A} to remove \mathcal{O} 's watermark.

Effect of key images. We observed that WM_{exp} is the only robust algorithm against evasion attacks. Note that WM_{exp} employs images selected from the same distribution as normal training instances for key images, while the other watermarking algorithms use out-of-distribution images.

Considering these two factors that affect the watermark robustness, we propose the following recommendations for improving its robustness. First, it is better to assign a single target label to all key images rather than random labels. Second, it is better to select key images from the same distribution as a regular training set rather than from a different distribution.

8.2 Suggestions for Adversarial Evaluation

From our evaluations, we draw the following takeaways that future research on designing a secure watermarking algorithm should consider. We encourage researchers to evaluate their defenses following our suggestions discussed herein, thus demonstrating a meaningful upper bound on their robustness.

Apply the complete attack set. We found out that all the previous works were broken by already existing attacks. They could have known this result if they have conducted a complete set of existing state-of-the-art attacks to evaluate their algorithms. In this regard, we suggest future research conduct at least a complete set of existing state-of-the-art attacks.

Use adaptive attacks. All the state-of-the-art watermarking algorithms were vulnerable to the proposed adaptive attacks. We believe that our adaptive attacks serve as a better baseline for demonstrating the robustness of a target watermarking scheme. We recommend future research to consider the proposed adaptive attacks when conducting fine-tuning, model stealing, and pruning attacks.

Focus on attacks that obscure \mathcal{O} 's ownership. Recall from §5.3.1 that an attack scenario in which the adversary conducts a single attack that claims her ownership is futile. Therefore, when evaluating attacks that aim to claim \mathcal{A} 's ownership, one should first launch attacks that remove \mathcal{O} 's watermark and then initiate the attacks to claim \mathcal{A} 's ownership.

Search for effective attack hyperparameters. Surprisingly, five out of the 10 evaluated watermarking algorithms were

Table 9: Summary of the attack results. ✓ denotes that the attack succeeded against a target model watermarked with the corresponding algorithm, whereas ✗ indicates that the attack failed. For each watermarking scheme, the successful attacks are presented in the order of MNIST, GTSRB, CIFAR-10, and CIFAR-100 models.

Attack (Adv.)	$WM_{content}$	WM_{noise}	$WM_{unrelated}$	WM_{mark}	$WM_{abstract}$	WM_{adv}	$WM_{passport}$	$WM_{encoder}$	WM_{exp}	DeepSigns
Fine-tuning (non-adap.)	✓✓✓✗	✓✗✗✗	✗✗✗✗	✓✓✓✓	✓✓✓✗	✓✓✓✗	✓✓✗✗	✓✓✓✗	✓✓✓✗	✓✓✓✓
Fine-tuning (adap.)	✓✓✓✗	✓✓✓✗	✓✗✓✗	✓✓✓✗	✓✗✗✗	✓✓✓✓	✓✓✗✗	✓✓✓✗	✓✓✓✗	✓✓✓✓
Stealing (non-adap.)	✗✓✓✗	✓✓✓✗	✗✗✗✗	✓✓✓✗	✓✓✓✗	✓✓✓✗	✓✓✗✗	✓✓✓✗	✓✓✓✗	✓✓✓✗
Stealing (adap.)	✓✓✓✗	✓✓✓✗	✓✗✓✗	✓✓✓✗	✓✓✓✗	✓✓✓✗	✓✓✗✗	✓✓✓✗	✓✓✓✗	✓✓✓✗
Pruning (non-adap.)	✗✗✗✗	✗✗✗✗	✗✗✗✗	✗✗✗✗	✓✗✗✗	✗✗✗✗	✓✗✓✗	✗✗✗✗	✗✗✗✗	✓✗✗✗
Pruning (adap.)	✓✗✗✗	✗✗✗✗	✓✗✗✗	✓✗✗✗	✓✗✗✗	✗✗✗✗	✗✗✗✗	✗✗✗✗	✗✗✗✗	✗✗✗✗
Evasion	✓✓✓✓	✓✓✓✓	✓✓✓✓	✓✓✓✓	✓✓✓✓	✓✓✓✓	✓✓✓✓	✓✓✓✓	✓✓✓✓	✓✓✓✓
Ownership Piracy	✓✓✗✗	✓✓✗✗	✓✓✗✗	✓✓✓✓	✓✓✗✗	✓✓✓✓	✓✓✗✗	✓✓✗✗	✓✓✗✗	✓✓✓✓
Ambiguity	✗✓✓✗	✓✓✓✗	✗✗✗✗	✓✓✓✗	✓✓✓✗	✓✓✓✗	✓✗✗✗	✓✓✓✗	✓✗✗✗	✓✓✓✗
# of Succeeded Attacks	6 7 6 1	7 7 5 1	5 2 2 1	8 7 7 2	9 6 5 0	7 7 7 2	8 5 1 0	7 7 6 1	6 6 5 0	8 7 7 3
Maximum # per Scheme	7	7	5	8	9	7	8	7	6	8

broken by attacks that the previous studies already evaluated (recall §7.3.1 and §7.3.4). To avoid providing a misleading upper bound on the robustness, follow-on research must conduct strong attacks by carefully exploring hyperparameters and adopting state-of-the-art attacks.

Consider diverse datasets. Overall, the models trained on the MNIST dataset tend to be vulnerable, as shown in Table 9. Interestingly, the watermarked models trained on CIFAR-100 were robust against the presented attacks in general. This is because the conducted attacks have always contributed decreasing a test accuracy over 5% (§E), which means that the presented attacks on the CIFAR-100 models easily undermine the models’ performance. We concluded that the over-parameterization for remembering the trigger sets of the CIFAR-100 models contributes to losing the models’ generality. Note that it is well-known that various DNN defense algorithms showed different levels of robustness depending on the dataset [7]. We thus suggest considering more datasets than the MNIST and CIFAR datasets when evaluating watermarking algorithms.

9 Related Work

Backdoor attacks. There have been several studies on backdoor attacks against DNN models [12, 24]. In this type of attack, a user sends a training set to the adversarial trainer to outsource the training process. The adversary then trains a model with the received normal data as well as images containing a backdoor trigger, e.g., a sticker with a flower. The goal of the adversary here is to lead the model to misclassify when the backdoor-triggering input is provided.

To mitigate backdoor attacks, researchers have proposed several mitigation methodologies [10, 34, 56]. DeepIn-

spect [10] reverse-engineers the backdoor trigger using a conditional generative model and then fine-tunes the target model by harnessing the generated backdoor-triggering images and their correct labels. Wang *et al.* [56] suggested another method that remedies the target model by removing neurons that contribute to misclassifying backdoor-triggering images.

Note that these defenses are similar to our adaptive fine-tuning attacks and adaptive pruning attacks *per se*. However, their approaches are not directly applicable to reverse-engineering key images of various trigger set-based DNN watermarking algorithms because they only focus on backdoor-triggering inputs created by adding a backdoor trigger to the source images. On the other hand, we demonstrated how an adaptive adversary generates key images against diverse watermarking schemes.

Adversarial example attacks. DNN models are known to misclassify adversarial examples created by adding quasi-imperceptible perturbations to normal examples [22, 50]. Since this finding, there has been a vast volume of research on adversarial examples. To mitigate this threat, Papernot *et al.* [41] proposed defensive distillation to smooth the network gradients exploited for generating adversarial samples. Other studies have aimed to detect such examples during the testing phase. Metzen *et al.* [37] trained a DNN binary classifier that distinguishes regular data from adversarial data. MagNet [35] detects and reforms adversarial examples by leveraging autoencoders trained on regular images. However, these defenses were later broken by other strong attacks [7–9]. In our study, we selected WM_{adv} that utilizes adversarial examples as our target watermarking scheme and employed the approach of MagNet for evasion attacks.

Model stealing attacks. The goal of model stealing attacks, also known as model extraction attacks, is to copy the classification performance of remote target models [53]. Paper-

not *et al.* [40] trained a counterfeit model as a stepping stone for creating adversarial examples of remote target models. Orekondy *et al.* [39] demonstrated that model stealing is still possible against complex DNN models even though the adversary does not have enough training sets and does not know the model structure. They showed that arbitrary images downloaded from the Internet and arbitrary models are enough to forge the target model. PRADA [29] detects model stealing attempts by analyzing incoming queries. However, this defense is inapplicable to DNN watermarking algorithms. Note that the adversary does not have to send remote queries because the target model is already in the hands of the adversary. We leveraged this attack for removing O 's watermark in the target model. In our settings, we prepared the training set for model stealing attacks in §7.3.2 following the approach of [39].

10 Conclusion

We investigate the current practice of demonstrating watermark robustness via adversarial evaluation in the previous studies. We point out two common flaws in their evaluations: (1) incomplete adversarial evaluation and (2) overlooked adaptive attacks. Taking into account these shortcomings, we evaluate the 10 trigger set-based watermarking schemes and demonstrate that every proposed watermarking scheme is vulnerable to at least five presented attacks, which significantly undermines their intended goal of proving ownership. We conclude these failures stem from the today's flawed practice in conducting adversarial evaluation. We encourage future studies on new watermarking algorithms to consider our guidelines presented herein to demonstrate a meaningful upper bound of the robustness against the complete set of the existing attacks, including the proposed adaptive attacks.

References

- [1] Martín Abadi, Ashish Agarwal, Paul Barham, Eugene Brevdo, Zhifeng Chen, Craig Citro, Greg S. Corrado, Andy Davis, Jeffrey Dean, Matthieu Devin, Sanjay Ghemawat, Ian Goodfellow, Andrew Harp, Geoffrey Irving, Michael Isard, Yangqing Jia, Rafal Jozefowicz, Lukasz Kaiser, Manjunath Kudlur, Josh Levenberg, Dandelion Mané, Rajat Monga, Sherry Moore, Derek Murray, Chris Olah, Mike Schuster, Jonathon Shlens, Benoit Steiner, Ilya Sutskever, Kunal Talwar, Paul Tucker, Vincent Vanhoucke, Vijay Vasudevan, Fernanda Viégas, Oriol Vinyals, Pete Warden, Martin Wattenberg, Martin Wicke, Yuan Yu, and Xiaoqiang Zheng. TensorFlow: Large-scale machine learning on heterogeneous systems. <https://www.tensorflow.org/>, 2015.
- [2] André Adelsbach, Stefan Katzenbeisser, and Helmut Veith. Watermarking schemes provably secure against copy and ambiguity attacks. In *Proceedings of the ACM Workshop on Digital Rights Management*, pages 111–119, 2003.
- [3] Yossi Adi, Carsten Baum, Moustapha Cisse, Benny Pinkas, and Joseph Keshet. Turning your weakness into a strength: Watermarking deep neural networks by backdooring. In *Proceedings of the USENIX Security Symposium*, pages 1615–1631, 2018.
- [4] Osbert Bastani, Yani Ioannou, Leonidas Lampropoulos, Dimitrios Vytiniotis, Aditya V. Nori, and Antonio Criminisi. Measuring neural net robustness with constraints. In *Proceedings of the Advances in Neural Information Processing Systems*, pages 2621–2629, 2016.
- [5] Xiaoyu Cao, Minghong Fang, Jia Liu, and Neil Zhenqiang Gong. FLTrust: Byzantine-robust federated learning via trust bootstrapping. In *Proceedings of the Network and Distributed System Security Symposium*, 2021.
- [6] Nicholas Carlini, Anish Athalye, Nicolas Papernot, Wieland Brendel, Jonas Rauber, Dimitris Tsipras, Ian Goodfellow, Aleksander Madry, and Alexey Kurakin. On evaluating adversarial robustness. *CoRR*, abs/1902.06705, 2019.
- [7] Nicholas Carlini and David Wagner. Adversarial examples are not easily detected: Bypassing ten detection methods. In *Proceedings of the ACM Workshop on Artificial Intelligence and Security*, pages 3–14, 2017.
- [8] Nicholas Carlini and David Wagner. MagNet and “efficient defenses against adversarial attacks” are not robust to adversarial examples. *CoRR*, abs/1711.08478, 2017.
- [9] Nicholas Carlini and David Wagner. Towards evaluating the robustness of neural networks. In *Proceedings of the IEEE Symposium on Security and Privacy*, pages 39–57, 2017.
- [10] Huili Chen, Cheng Fu, Jishen Zhao, and Farinaz Koushanfar. DeepInspect: A black-box trojan detection and mitigation framework for deep neural networks. In *Proceedings of the International Joint Conference on Artificial Intelligence*, pages 4658–4664, 2019.
- [11] Huili Chen, Bitar Darvish Rouhani, Cheng Fu, Jishen Zhao, and Farinaz Koushanfar. DeepMarks: A secure fingerprinting framework for digital rights management of deep learning models. In *Proceedings of the ACM International Conference on Multimedia Retrieval*, pages 105–113, 2019.
- [12] Xinyun Chen, Chang Liu, Bo Li, Kimberly Lu, and Dawn Song. Targeted backdoor attacks on deep learning systems using data poisoning. *CoRR*, abs/1712.05526, 2017.

- [13] Xinyun Chen, Wenxiao Wang, Chris Bender, Yiming Ding, Ruoxi Jia, Bo Li, and Dawn Song. REFIT: a unified watermark removal framework for deep learning systems with limited data. *CoRR*, abs/1911.07205, 2019.
- [14] Yizheng Chen, Shiqi Wang, Dongdong She, and Suman Jana. On training robust PDF malware classifiers. In *Proceedings of the USENIX Security Symposium*, pages 2343–2360, 2020.
- [15] François Chollet and Others. Keras. <https://keras.io>, 2015.
- [16] Anna Choromanska, Mikael Henaff, Michael Mathieu, Gerard Ben Arous, and Yann LeCun. The loss surfaces of multilayer networks. In *Proceedings of the International Conference on Artificial Intelligence and Statistics*, pages 192–204, 2015.
- [17] Scott Craver, Nasir Memon, Boon-Lock Yeo, and Minerva M. Yeung. Resolving rightful ownerships with invisible watermarking techniques: Limitations, attacks, and implications. *IEEE Journal on Selected Areas in Communications*, 16(4):573–586, 1998.
- [18] Yue Deng, Feng Bao, Youyong Kong, Zhiqian Ren, and Qionghai Dai. Deep direct reinforcement learning for financial signal representation and trading. *IEEE Transactions on Neural Networks and Learning Systems*, 28(3):653–664, 2017.
- [19] Lixin Fan, Kam Woh Ng, and Chee Seng Chan. Rethinking deep neural network ownership verification: Embedding passports to defeat ambiguity attacks. In *Proceedings of the Advances in Neural Information Processing Systems*, pages 4716–4725, 2019.
- [20] Thomas Fischer and Christopher Krauss. Deep learning with long short-term memory networks for financial market predictions. *European Journal of Operational Research*, 270(2):654–669, 2018.
- [21] Matt Fredrikson, Somesh Jha, and Thomas Ristenpart. Model inversion attacks that exploit confidence information and basic countermeasures. In *Proceedings of the ACM Conference on Computer and Communications Security*, pages 1322–1333, 2015.
- [22] Ian J. Goodfellow, Jonathon Shlens, and Christian Szegedy. Explaining and harnessing adversarial examples. In *Proceedings of the International Conference on Learning Representations*, 2015.
- [23] Albert Gordo, Jon Almazán, Jerome Revaud, and Diane Larlus. Deep image retrieval: Learning global representations for image search. In *Proceedings of the European Conference on Computer Vision*, pages 241–257, 2016.
- [24] Tianyu Gu, Brendan Dolan-Gavitt, and Siddharth Garg. BadNets: Identifying vulnerabilities in the machine learning model supply chain. *CoRR*, abs/1708.06733, 2019.
- [25] Jia Guo and Miodrag Potkonjak. Watermarking deep neural networks for embedded systems. In *Proceedings of the IEEE/ACM International Conference on Computer-Aided Design*, pages 1–8, 2018.
- [26] Kaiming He, Xiangyu Zhang, Shaoqing Ren, and Jian Sun. Deep residual learning for image recognition. In *Proceedings of the IEEE Conference on Computer Vision and Pattern Recognition*, pages 770–778, 2016.
- [27] Xiaowei Huang, Marta Kwiatkowska, Sen Wang, and Min Wu. Safety verification of deep neural networks. In *Proceedings of the International Conference on Computer Aided Verification*, pages 3–29, 2017.
- [28] Jinyuan Jia, Ahmed Salem, Michael Backes, Yang Zhang, and Neil Zhenqiang Gong. MemGuard: Defending against black-box membership inference attacks via adversarial examples. In *Proceedings of the ACM Conference on Computer and Communications Security*, pages 259–274, 2019.
- [29] Mika Juuti, Sebastian Szyller, Samuel Marchal, and N. Asokan. PRADA: Protecting against DNN model stealing attacks. In *Proceedings of the IEEE European Symposium on Security and Privacy*, pages 512–527, 2019.
- [30] Diederik P. Kingma and Jimmy Ba. Adam: A method for stochastic optimization. In *Proceedings of the International Conference on Learning Representations*, 2015.
- [31] Gerhard C. Langelaar, Iwan Setyawan, and Reginald L. Lagendijk. Watermarking digital image and video data. a state-of-the-art overview. *IEEE Signal Processing Magazine*, 17(5):20–46, 2000.
- [32] Yann LeCun, Léon Bottou, Yoshua Bengio, and Patrick Haffner. Gradient-based learning applied to document recognition. In *Proceedings of the IEEE*, pages 2278–2324, 1998.
- [33] Zheng Li, Chengyu Hu, Yang Zhang, and Shanqing Guo. How to prove your model belongs to you: A blind-watermark based framework to protect intellectual property of DNN. In *Proceedings of the Annual Computer Security Applications Conference*, pages 126–137, 2019.
- [34] Yingqi Liu, Wen-Chuan Lee, Guan hong Tao, Shiqing Ma, Yousra Aafer, and Xiangyu Zhang. ABS: Scanning neural networks for back-doors by artificial brain

- stimulation. In *Proceedings of the ACM Conference on Computer and Communications Security*, pages 1265–1282, 2019.
- [35] Dongyu Meng and Hao Chen. MagNet: a two-pronged defense against adversarial examples. In *Proceedings of the ACM Conference on Computer and Communications Security*, pages 135–147, 2017.
- [36] Erwan Le Merrer, Patrick Pérez, and Gilles Trédan. Adversarial frontier stitching for remote neural network watermarking. *Neural Computing and Applications*, 2019.
- [37] Jan Hendrik Metzen, Tim Genewein, Volker Fischer, and Bastian Bischoff. On detecting adversarial perturbations. In *Proceedings of the International Conference on Learning Representations*, 2017.
- [38] Ryota Namba and Jun Sakuma. Robust watermarking of neural network with exponential weighting. In *Proceedings of the ACM Asia Conference on Computer and Communications Security*, pages 228–240, 2019.
- [39] Tribhuvanesh Orekondy, Bernt Schiele, and Mario Fritz. Knockoff nets: Stealing functionality of black-box models. In *Proceedings of the IEEE Conference on Computer Vision and Pattern Recognition*, pages 4954–4963, 2019.
- [40] Nicolas Papernot, Patrick McDaniel, Ian Goodfellow, Somesh Jha, Z. Berkay Celik, and Ananthram Swami. Practical black-box attacks against machine learning. In *Proceedings of the ACM Asia Conference on Computer and Communications Security*, pages 506–519, 2017.
- [41] Nicolas Papernot, Patrick McDaniel, Xi Wu, Somesh Jha, and Ananthram Swami. Distillation as a defense to adversarial perturbations against deep neural networks. In *Proceedings of the IEEE Symposium on Security and Privacy*, pages 582–597, 2016.
- [42] Erwin Quiring, David Klein, Daniel Arp, Martin Johns, and Konrad Rieck. Adversarial preprocessing: Understanding and preventing image-scaling attacks in machine learning. In *Proceedings of the USENIX Security Symposium*, pages 1363–1380, 2020.
- [43] Olaf Ronneberger, Philipp Fischer, and Thomas Brox. U-Net: Convolutional networks for biomedical image segmentation. In *Proceedings of the International Conference on Medical Image Computing and Computer-Assisted Intervention*, pages 234–241, 2015.
- [44] Bitva Darvish Rouhani, Huili Chen, and Farinaz Koushanfar. DeepSigns: An end-to-end watermarking framework for ownership protection of deep neural networks. In *Proceedings of the ACM International Conference on Architectural Support for Programming Languages and Operating Systems*, pages 485–497, 2019.
- [45] Olga Russakovsky, Jia Deng, Hao Su, Jonathan Krause, Sanjeev Satheesh, Sean Ma, Zhiheng Huang, Andrej Karpathy, Aditya Khosla, Michael Bernstein, Alexander C. Berg, and Li Fei-Fei. ImageNet large scale visual recognition challenge. *International Journal of Computer Vision*, 115(3):211–252, 2019.
- [46] Uri Shaham, Yutaro Yamada, and Sahand Negahban. Understanding adversarial training: Increasing local stability of neural nets through robust optimization. *CoRR*, abs/1511.05432, 2016.
- [47] Shawn Shan, Emily Wenger, Bolun Wang, Bo Li, Haitao Zheng, and Ben Y. Zhao. Gotta catch ’em all: Using honeypots to catch adversarial attacks on neural networks. In *Proceedings of the ACM Conference on Computer and Communications Security*, pages 67–83, 2020.
- [48] Ashish Shrivastava, Tomas Pfister, Oncel Tuzel, Joshua Susskind, Wenda Wang, and Russell Webb. Learning from simulated and unsupervised images through adversarial training. In *Proceedings of the IEEE Conference on Computer Vision and Pattern Recognition*, pages 2107–2116, 2017.
- [49] Mitchell D. Swanson, Mei Kobayashi, and Ahmed H. Tewfik. Multimedia data-embedding and watermarking technologies. *Proceedings of the IEEE*, 86(6):1064–1087, 1998.
- [50] Christian Szegedy, Wojciech Zaremba, Ilya Sutskever, Joan Bruna, Dumitru Erhan, Ian Goodfellow, and Rob Fergus. Intriguing properties of neural networks. In *Proceedings of the International Conference on Learning Representations*, 2014.
- [51] PyTorch Core Team. Pytorch. <https://pytorch.org/>.
- [52] Yuchi Tian, Kexin Pei, Suman Jana, and Baishakhi Ray. DeepTest: Automated testing of deep-neural-network-driven autonomous cars. In *Proceedings of the International Conference on Software Engineering*, pages 303–314, 2018.
- [53] Florian Tramér, Fan Zhang, Ari Juels, Michael K. Reiter, and Thomas Ristenpart. Stealing machine learning models via prediction APIs. In *Proceedings of the USENIX Security Symposium*, pages 601–618, 2016.
- [54] Yusuke Uchida, Yuki Nagai, Shigeyuki Sakazawa, and Shin’ichi Satoh. Embedding watermarks into deep neural networks. In *Proceedings of the ACM International Conference on Multimedia Retrieval*, pages 269–277, 2017.

- [55] Ji Wan, Dayong Wang, Steven C.H. Hoi, Pengcheng Wu, Jinake Zhu, Yongdong Zhang, and Jintao Li. Deep learning for content-based image retrieval: A comprehensive study. In *Proceedings of the ACM International Conference on Multimedia*, pages 157–166, 2016.
- [56] Bolun Wang, Yuanshun Yao, Shawn Shan, Huiying Li, Bimal Viswanath, Haitao Zheng, and Ben Y. Zhao. Neural Cleanse: Identifying and mitigating backdoor attacks in neural networks. In *Proceedings of the IEEE Symposium on Security and Privacy*, pages 707–723, 2019.
- [57] Han Xiao, Kashif Rasul, and Roland Vollgraf. Fashion-MNIST: a novel image dataset for benchmarking machine learning algorithms. *CoRR*, abs/1708.07747, 2017.
- [58] Xiaojun Xu, Chang Liu, Qian Feng, Heng Yin, Le Song, and Dawn Song. Neural network-based graph embedding for cross-platform binary code similarity detection. In *Proceedings of the ACM Conference on Computer and Communications Security*, pages 363–376, 2017.
- [59] Guixin Ye, Zhanyong Tang, Dingyi Fang, Zhanxing Zhu, Yansong Feng, Pengfei Xu, Xiaojiang Chen, and Zheng Wang. Yet another text captcha solver: A generative adversarial network based approach. In *Proceedings of the ACM Conference on Computer and Communications Security*, pages 332–348, 2018.
- [60] Chiyuan Zhang, Samy Bengio, Moritz Hardt, Benjamin Recht, and Oriol Vinyals. Understanding deep learning requires rethinking generalization. In *Proceedings of the International Conference on Learning Representations*, 2017.
- [61] Jialong Zhang, Zhongshu Gu, Jiyong Jang, Hui Wu, Marc Ph. Stoecklin, Heqing Huang, and Ian Molloy. Protecting intellectual property of deep neural networks with watermarking. In *Proceedings of the ACM Asia Conference on Computer and Communications Security*, pages 159–172, 2018.
- [62] Jie Zhang, Dongdong Chen, Jing Liao, Han Fang, Weiming Zhang, Wenbo Zhou, Hao Cui, and Nenghai Yu. Model watermarking for image processing networks. In *Proceedings of the AAAI Conference on Artificial Intelligence*, 2020.

A Target Watermark Schemes

We describe 10 of the selected representative watermarking algorithms that leverage a trigger set. For ease of explanation, we leverage Algorithm 1 (§2.2) to explain key procedures that differ in each watermarking scheme.

A.1 Embedding Meaningful Content ($WM_{content}$) or Noise (WM_{noise}) into Images

Zhang *et al.* [61] proposed a watermarking algorithm for a target model to learn the relationships between a target label and key images embedding meaningful content or noises. Specifically, in their watermarking algorithm, the `EmbedWatermark` function takes source images of a given class from a training set. The `GenerateKeyImgs` function superimposes either extra meaningful content, such as a textual image with the word: “TEST,” or a Gaussian noise onto source images. The `AssignKeyLabels` function selects one class other than the given source class and assigns this class to all the superimposed key images. This new class is called a *target label*. At last, the `TrainModel` function trains a model with both the trigger and original training sets from scratch.

A.2 Using an Unrelated Class of Images ($WM_{unrelated}$)

Zhang *et al.* [61] also proposed another way of leveraging images unrelated to the original purpose of a target DNN model. In this scheme, a model owner O chooses a target label and then trains source images of which class is unrelated to this target label. Assume that O builds a food DNN classifier, she picks a “hamburger” target label and trains airplane images with this target label, thus rendering the airplane images as the watermark key images. That is, O takes key images from a distinct distribution rather than synthesizing new images from the original training set.

A.3 Embedding a Message Mark into Images (WM_{mark})

Guo *et al.* [25] designed the `GenerateKeyImgs` function to synthesize key images by adding noise and the `AssignKeyLabels` function to assign labels to the synthesized images. The proposed method is not quite different from embedding a Gaussian noise (§A.1), but this approach differs in that the noise and target labels are devised to incorporate the signature of a model owner. The `TrainModel` function trains a model with a regular training set and then fine-tunes the model using both the regular set and trigger set to embed watermarks.

A.4 Using a Set of Abstract Images ($WM_{abstract}$)

Adi *et al.* [3] suggested an approach that uses abstract images as key images without relying on the `GenerateKeyImgs` function. The `AssignKeyLabels` function then randomly allocates a class to each abstract image. To train a model, the `TrainModel` function uses both the regular training set and trigger set. Their approach is similar to the aforementioned approach using an unrelated class of images because it leverages images taken from a distinct distribution different to that of the original training set. However, the key difference is that they devised a secure verification procedure.

When deploying a model, O provides a *public verification key*, the encrypted version of a trigger set. The verification procedure involves a trusted third party. This trusted verifier asks O or an adversary to submit an *encryption key* and the trigger set, together called a *private marking key*. The verifier first checks whether the public key can be decrypted with the submitted encryption key. If so, the verifier then checks whether the decrypted key images trigger their corresponding target labels.

A.5 Watermarking via Adversarial Training (WM_{adv})

Merrer *et al.* [36] utilized adversarial examples as key images. The `GenerateKeyImgs` function runs FGSM [22] on a pre-trained model to create adversarial examples that yield misclassification of the model. Then, `AssignKeyLabels` labels each created example with a ground-truth class, and `TrainModel` fine-tunes the pre-trained model with these pairs in addition to the regular training data.

This approach is analogous to adversarial training [22, 46] in that a model watermarked with WM_{adv} becomes robust against such adversarial examples. On the other hand, unwatermarked models are still vulnerable to these examples, due to the transferability of adversarial examples [22]. The original owner of a model can verify her ownership by leveraging this difference.

A.6 Embedding Passports into DNNs ($WM_{passport}$)

Fan *et al.* [19] proposed a novel model structure to hinder ambiguity attacks that aim to extract key images. They focused on building a secure model architecture instead of devising secure key images. In `TrainModel`, they proposed to add security layers, called *passport layers*, instead of convolutional layers in a model. Other functions work in the same way as the approach by Adi *et al.* [3].

A passport layer takes in as inputs a user-provided passport and an output from the previous layer. Note that the output of a passport layer is only meaningful when a valid passport,

which was provided in a training phase, is given. Thus, valid passports need to be kept secret for unauthorized users in this approach, and model owners O may want to hide the passport layers when deploying their models. For the sake of achieving this goal, the restructured model is trained in a way to decrease both (1) the original loss when no passport layers are inserted and (2) the new loss when the passport layers are inserted. After this multi-task training, the model can be distributed without the passport layers because the model is trained to perform inference with and without the passport layers.

To prove ownership, the owner attempts to verify ownership by querying a suspicious model with key images. If the model returns predefined labels, the user can ask white-box access to the model with help of law enforcement and check whether the key images still trigger the predefined labels even when the passport layers are added back to the model.

A.7 Synthesizing Watermark Images with an Encoder ($WM_{encoder}$)

Li *et al.* [33] focused on generating key images that have a distribution similar to that of the original training set. Given source images, the `GenerateKeyImgs` function uses encoder and discriminator networks to reconstruct source images, and the reconstructed images become key images, thus rendering these key images to have a similar distribution to their original ones. For each key image, the `AssignKeyLabels` function then randomly allocates a class to each abstract image. The remaining functions work the same as those proposed by Adi *et al.* [3].

The proposed scheme is designed to prevent evasion attacks. An evasion attack is an attempt for an adversary to discard any inquiry with genuine key images, which prevent a legitimate model owner from proving the ownership. Generating key images similar to their original ones causes the adversary difficult to distinguish key images.

A.8 Training with Exponential Weighting (WM_{exp})

Namba *et al.* [38] designed a watermarking algorithm that mitigates parameter pruning and evasion attacks. In their algorithm, the `GenerateKeyImgs` function takes key images from a regular training set. Since these images share the same distribution with normal images, an adversary is highly likely to fail at distinguishing them.

After `AssignKeyLabels` assigns a label other than the ground-truth label to each selected key image, the `TrainModel` function fine-tunes a pre-trained model with exponential weighting. The intuition behind this approach is that we can exponentially increase weight parameters that contribute to the model’s prediction, thus hardening the em-

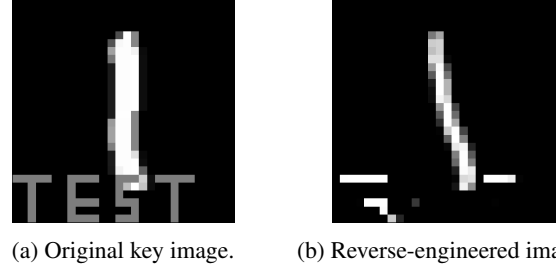


Figure 3: Examples of O ’s key image and reverse-engineered key image ($WM_{content}$).

bedded watermarks against pruning attacks that aim to remove small weights.

A.9 Implanting a Random Trigger Set (DeepSigns)

DeepSigns [44] randomly creates key images and their target labels. Specifically, it generates a random trigger set such that a pre-trained model fails to predict the target labels but becomes able to correctly predict after fine-tuning. Thus, the owner can send a query with the created key images for verifying her ownership.

B Adaptive Attacks

We demonstrate how an adversary adaptively creates a trigger set against a given watermarking scheme, which aims at unlearning O ’s original trigger set. Specifically, we explain loss functions and source images that we leveraged to train autoencoders. For the autoencoder architectures, we adopted a ResNet18-based U-Net model for $WM_{passport}$ and a regular U-Net model [43] for the other schemes.

Remind that we conducted fine-tuning, model stealing, and parameter pruning adaptive attacks against the 10 watermark schemes (§7.3.1, §7.3.2, and §7.3.3). For this, we have devised 30 different adaptive attacks (3 attacks \times 10 schemes). Instead of explaining each adaptive attack, we categorize the target watermarking schemes into two groups according to the internal working of `GenerateKeyImgs` and then explain the generation of key images using the autoencoder for each group.

Among our 10 target watermarking algorithms, $WM_{content}$, WM_{noise} , and WM_{mark} create key images by superimposing content, noise, or mark onto source images, respectively. On the other hand, the remaining seven watermarking schemes take key images from the same or dissimilar distributions.

B.1 Superimposing One Image onto Another

Embedding content ($WM_{content}$). We first define a key image x' that includes a content image C on top of a source image x

as follows:

$$x' = (1 - \mathcal{M}) \cdot x + \mathcal{M} \cdot C \quad (2)$$

Here, \mathcal{M} represents a mask that determines how much C overlaps with x , similar to the approach of Wang *et al.* [56].

To model the GenerateKeyImgs function of $WM_{content}$, we employ two autoencoders, each of which is specially designed to generate C and \mathcal{M} , respectively. Note that x' in $WM_{content}$ contains concise content, as shown in Figure 3a. In other words, \mathcal{M} should be sufficiently small enough to overlay only a small portion of x .

Incorporating all these together, we trained two autoencoders with the random content C and the random mask \mathcal{M} such that (1) the generated content C' does not significantly differ from C and (2) the created mask \mathcal{M}' remains sufficiently small. Specifically, we designed the following loss function as L_{ae} in Equation 1.

$$L_{ae} = \text{MSE}(C, C') + \gamma \cdot |\mathcal{M}'| \quad (3)$$

In Equation 3, the first term computes mean squared errors between C and C' , and the second term refers to the L_1 norm of \mathcal{M}' .

Once each autoencoder outputs C' and \mathcal{M}' , they are combined with source images x as in Equation 2, thus becoming the reverse-engineered key images x' . Then, these reverse-engineered images are provided to M_{wm} for computing the classification error loss term in Equation 1. As the source images, we used 50% of a test set. Figure 3b shows a reverse-engineered image x' after training. Note that the content of this image resembles that of Figure 3a.

Embedding noise or mark (WM_{noise} or WM_{mark}). A key image x' is defined as the following where Z indicates noise or mark embedded in a source image x .

$$x' = x + Z \quad (4)$$

To model how WM_{noise} and WM_{mark} generate these key images, we organized an autoencoder to create Z , which is added to the source image x .

Note that the training objective of this autoencoder is to modify Z so that the output noise Z' can cause the misclassification of M_{wm} when added to x . At the same time, \mathcal{A} aims to make Z' remain close to the noise or mark generated with the given watermarking algorithm. To this end, we harnessed the mean squared error between Z and Z' as L_{ae} and trained the autoencoder with random noise Z created by following the given watermarking algorithm. We used 50% of a test set as the source images for training the autoencoder, as we did for $WM_{content}$.

B.2 Collecting Images from the Distribution

Images from the same or similar distribution (WM_{exp} or $WM_{encoder}$). Recall that WM_{exp} takes a small subset of a training set and uses it as key images; $WM_{encoder}$ aims to create

key images that are close to the images used for training M_{wm} . In other words, both watermarking schemes seek to design key images that are indistinguishable from the images used for training. Therefore, we directly trained the autoencoder to output key images x' such that x' is close to the source images x , which is 50% of a test set. Specifically, we trained the autoencoder in the direction of minimizing the mean squared error between x and x' .

To further improve the autoencoder’s ability of placing x' close to x , we also trained a discriminator network D that outputs whether the given image is a real image. Following the general GAN approach [48], we alternated training between the autoencoder and discriminator so that the autoencoder can gradually improve the output images x' enough to fool the discriminator as training proceeds. When training the autoencoder, we used the following objective function as L_{ae} in Equation 1.

$$L_{ae} = \text{MSE}(x, x') + \gamma \cdot L_{dis}(x', 0) \quad (5)$$

Here, the first term corresponds to the mean squared error function, and the second term is the classification error of the discriminator network. Note that the discriminator network is trained to output 1 for real images and 0 for synthesized images. Therefore, the second term is designed to create x' that is able to fool the discriminator network.

Adversarial examples (WM_{adv}). Since WM_{adv} crafts adversarial examples to use as key images, the adaptive adversary can simply simulate the GenerateKeyImgs function without the autoencoder. That is, the adversary can create adversarial examples without training the autoencoder. We used 50% of a test set for creating adversarial examples x' .

Images from the dissimilar distribution. The remaining four watermarking schemes collect or generate the out-of-distribution images as key images. We thus prepared random source images following each watermarking scheme and trained the autoencoder to reduce the mean squared errors between the source and synthesized images.

We prepared the following source images for each watermarking algorithm. We prepared random abstract images for training the autoencoder against $WM_{abstract}$ and $WM_{passport}$. When training the autoencoder against DeepSigns, we provided randomly created images to the autoencoder. Lastly, for $WM_{unrelated}$, we collected arbitrary images that belong to a single unrelated class.

C Experimental Results Different to Previous Studies

We demonstrated that WM_{noise} , $WM_{abstract}$, $WM_{passport}$, $WM_{encoder}$, and DeepSigns do not withstand fine-tuning and evasion attacks (§7.3.1 and §7.3.4), even though previous studies already demonstrated their robustness against those

Table 10: Performance of M_{adv} after fine-tuning attacks with various settings.

Optim.	Dataset	Lr	Trigger Set Recall (%)		Δ Test Acc. (%)	
			C10	C100	C10	C100
SGD	Train	0.0005	100	100	0.10	0.24
Adam	Train	0.0005	75.00	66.00	-3.40	-7.30
Adam	Test \cup Random	0.0005	60.00	26.00	-4.16	-8.20
Adam	Test \cup Random	0.001	26.00	6.00	-8.20	-11.54

attacks. In this section, we present that these different experimental results stem from (1) different attack settings that the adversary is able to arrange and (2) a weak attack that does not represent a meaningful upper bound on the watermark robustness.

Fine-tuning attack. When conducting fine-tuning attacks, there exist three factors that affect attack results: optimizer, dataset, and learning rate. To investigate the effect of these factors, we conducted fine-tuning attacks with various settings against M_{wm} watermarked with $WM_{abstract}$. We chose $WM_{abstract}$ because the previous study [3] provided detailed descriptions on how they conducted fine-tuning attacks. We only considered M_{wm} trained with CIFAR-10 and CIFAR-100 because the previous study did not evaluate M_{wm} trained with MNIST and GTSRB.

Table 10 summarizes the experimental results. The previous study conducted fine-tuning attacks with the settings in the first row. They fine-tuned M_{wm} with a stochastic gradient descent optimizer, the entire training set, and the last learning rate used for training M_{wm} . With this setting, the trigger set recalls did not drop at all, which accord with the previous study. However, as shown in the second row, when we optimize M_{wm} with Adam [30] during fine-tuning, the trigger set recalls decreased at least 25%. We confirmed that this also happens with the code released by the original paper.

As the third row represents, we further replaced the dataset for fine-tuning M_{wm} with 50% of a test set as well as randomly sampled unlabeled images. This is the same setting that we used in §7.3.1. The trigger set recalls dropped significantly in this setting. When conducting fine-tuning attacks in this setting against $WM_{abstract}$ with CIFAR-10, the adversary dropped the trigger set recall to be 60% with a slight drop of within 5% in test accuracy.

Note that the previous study assumes that the strong \mathcal{A} has access to the entire training set. They used this training set to make a target model forget its trigger set via conducting fine-tuning attacks. However, we believe that conducting the attacks with training instances that are disjointed from the original training set is more effective to achieve the adversary’s goal of decreasing a trigger set recall. The experimental result in the third row accords with this assumption.

Table 11: Performance of M_{adv} watermarked with DeepSigns assuming adversaries who have access to the different amount of a test set: (1) Trigger set recall (%) after fine-tuning and model stealing attacks, (2) Trigger set detection accuracy (%) after evasion attacks, and (3) Trigger set recall difference (%) between \mathcal{A} and \mathcal{O} after piracy and ambiguity attacks.

	10%				50%			
	MN	GT	C10	C100	MN	GT	C10	C100
Fine-tuning (non-adap.)	12.00	2.00	10.00	5.00	11.00	1.00	8.00	0.00
Fine-tuning (adap.)	9.00	4.00	11.00	2.00	11.00	1.00	12.00	2.00
Stealing (non-adap.)	10.00	0.00	11.00	1.00	10.00	3.00	6.00	1.00
Stealing (adap.)	14.00	4.00	11.00	0.00	6.00	2.00	11.00	0.00
Evasion	97.50	90.50	96.50	58.50	100	97.00	100	93.00
Piracy	84.00	98.00	77.00	99.00	88.00	98.00	92.00	100
Ambiguity	90.00	100	89.00	99.00	90.00	97.00	94.00	97.00

Finally, we evaluated whether increasing a learning rate affects the attack results. As shown in the last row, the trigger set recalls even further dropped under 30% at the cost of test accuracy drops.

We emphasize that the choice of an optimizer and a learning rate for fine-tuning attacks is completely up to the adversary. Therefore, the fine-tuning attacks conducted by the previous study was rather weak to demonstrate the robustness of their watermarks.

Evasion attack. There exist many approaches to detect images from a distribution other than the given one. That is, one can build a detector to distinguish key images from normal ones with various approaches. To build such a detector, WM_{exp} took a relatively weak approach; they devised a simple network by leveraging the former layers of ResNet-18 as a feature extractor and a fully connected layer as the output layer for binary classification. We note that they did not consider a sufficiently strong detection approach, such as Magnet [35], which was a state-of-the-art approach when the first watermarking scheme was suggested.

From these observations, we conclude that the previous studies have implemented relatively weak attacks, thus failing to demonstrate a meaningful upper bound on their robustness.

D Adversary with Fewer Data

Recall from §3.2 that we assumed an adversary who has access to 50% of a test set. We now relax this assumption and demonstrate whether an adversary with fewer data (i.e., 10% of a test set) can still successfully infringe on the IP of \mathcal{O} . Specifically, assuming this weaker adversary, we evaluate whether the performance of each attack degrades.

It is obvious that a watermarking algorithm that was robust under the original assumption would be still robust against the weaker attacks conducted by this adversary. Therefore, we evaluate whether DeepSigns, one of the most vulnerable

schemes, is able to withstand our attacks when we consider an adversary with fewer data (recall Table 9).

Table 11 summarizes the attack results. The left and right halves of the table illustrate the results from an adversary with 10% and 50% of a test set, respectively. We did not include non-adaptive and adaptive pruning attacks in the table because they do not use the test set for the attacks. Overall, the attack performance was not significantly affected by the amount of data to which the adversary has access. Each M_{wm} that was broken by the original adversary’s attacks was again destroyed by the weaker adversary. However, note in the table that the CIFAR-100 model was robust to the evasion attacks. Recall from §7.3.4 that we train the autoencoders for each class. Therefore, the attack failed as we did not have enough training instances for each of the 100 autoencoders.

E Expanded Tables

Tables 12–14 show the expanded versions of Tables 3–5, and Tables 15–16 correspond to Table 7–8, respectively. In addition to the trigger set recalls shown in the original tables, we included the magnitude of test accuracy drops in the expanded versions. Recall that we used 50% of a test set when mounting fine-tuning and model stealing attacks. Therefore, for these attacks, we computed the test accuracies with the remaining 50% of a test set that is disjoint from the set used for the attacks.

Table 12: Performance of M_{adv} after fine-tuning attacks.

	Non-adaptive Attack								Adaptive Attack							
	Trigger Set Recall (%)				Δ Test Acc. (%)				Trigger Set Recall (%)				Δ Test Acc. (%)			
	MNIST	GTSRB	C10	C100	MNIST	GTSRB	C10	C100	MNIST	GTSRB	C10	C100	MNIST	GTSRB	C10	C100
$WM_{content}$	57.02	0.36	24.54	13.20	-0.88	1.22	-3.94	-6.14	39.74	53.96	26.92	75.20	-1.40	2.83	-4.64	-9.70
WM_{noise}	5.93	84.46	99.14	93.80	-0.30	2.38	-4.38	-9.48	0.36	5.63	3.78	10.20	-1.46	-0.43	-4.42	-9.58
$WM_{unrelated}$	99.34	100	99.10	92.80	-1.32	2.45	-4.60	-7.74	32.76	99.77	17.26	0.00	-2.10	3.31	-4.36	-7.42
WM_{mark}	40.28	8.95	3.86	2.29	-1.12	-0.29	-3.76	-4.94	19.77	25.87	8.02	1.46	-2.72	1.03	-4.60	-8.20
$WM_{abstract}$	51.00	51.00	60.00	26.00	-0.86	1.65	-4.16	-8.20	45.00	83.00	54.00	23.00	-0.96	3.61	-3.96	-9.40
WM_{adv}	35.00	79.00	24.00	13.00	-1.38	0.70	-3.10	-5.82	14.00	8.00	12.00	2.00	-1.40	1.98	-2.20	-4.94
$WM_{passport}$	14.00	43.00	14.00	3.00	-1.04	2.95	-7.22	-10.06	13.00	43.00	17.00	3.00	-0.56	3.63	-6.52	-9.90
$WM_{encoder}$	20.00	4.08	20.00	8.00	-0.62	3.06	-4.04	-8.14	17.00	7.14	20.60	5.60	-1.32	4.69	-4.04	-8.30
WM_{exp}	6.00	0.00	1.00	1.00	-0.36	2.25	-4.12	-5.94	7.00	0.00	2.00	0.00	-0.46	4.42	-2.88	-6.74
DeepSigns	11.00	1.00	8.00	0.00	-1.46	1.08	-4.64	-4.98	11.00	1.00	12.00	2.00	-1.16	2.36	-2.88	-3.52

Table 13: Performance of M_{adv} after model stealing attacks.

	Non-adaptive Attack								Adaptive Attack							
	Trigger Set Recall (%)				Δ Test Acc. (%)				Trigger Set Recall (%)				Δ Test Acc. (%)			
	MNIST	GTSRB	C10	C100	MNIST	GTSRB	C10	C100	MNIST	GTSRB	C10	C100	MNIST	GTSRB	C10	C100
$WM_{content}$	82.94	0.00	2.04	0.80	-0.52	-1.68	-3.76	-10.64	28.37	0.05	1.18	0.40	-0.92	4.48	-3.54	-11.06
WM_{noise}	0.21	59.19	3.60	45.60	-0.44	-2.15	-4.02	-11.62	0.09	6.76	4.04	87.60	-1.34	4.02	-4.36	-12.64
$WM_{unrelated}$	99.76	100	95.26	0.00	-1.08	-0.51	-4.10	-11.08	34.94	100	9.02	0.00	-0.88	4.83	-4.50	-12.56
WM_{mark}	11.57	5.10	2.32	0.90	-0.82	1.06	-2.18	-6.54	7.66	7.27	6.81	1.46	-1.26	1.74	-2.76	-8.00
$WM_{abstract}$	41.00	35.00	24.00	2.00	-1.02	2.26	-3.90	-11.62	39.00	48.00	27.00	2.00	-0.72	4.40	-3.40	-12.76
WM_{adv}	23.00	70.00	8.00	11.00	-0.84	-1.33	-2.90	-8.36	17.00	0.00	16.00	1.00	-1.52	1.90	-3.26	-9.30
$WM_{passport}$	7.00	34.00	19.00	2.00	-0.36	5.24	-11.12	-17.62	7.00	37.00	16.00	1.00	-0.52	5.29	-9.66	-18.94
$WM_{encoder}$	9.67	2.55	12.60	1.80	-1.28	-1.08	-3.82	-11.76	9.33	2.30	13.20	1.40	-1.88	6.19	-4.60	-12.16
WM_{exp}	1.00	0.00	2.00	0.00	-1.34	2.34	-3.56	-9.40	4.00	0.00	2.00	2.00	-1.80	5.04	-3.92	-10.62
DeepSigns	10.00	3.00	6.00	1.00	-1.28	0.67	-2.68	-8.40	6.00	2.00	11.00	0.00	-1.52	3.31	-2.60	-8.84

Table 14: Performance of M_{adv} after parameter pruning attacks.

	Non-adaptive Attack								Adaptive Attack							
	Trigger Set Recall (%)				Δ Test Acc. (%)				Trigger Set Recall (%)				Δ Test Acc. (%)			
	MNIST	GTSRB	C10	C100	MNIST	GTSRB	C10	C100	MNIST	GTSRB	C10	C100	MNIST	GTSRB	C10	C100
$WM_{content}$	99.87	100	100	100	-0.12	0.06	0.00	0.03	64.95	100	100	100	-0.29	-7.65	0.00	-6.41
WM_{noise}	100	100	100	100	-0.01	0.01	0.00	0.00	97.29	0.27	100	58.20	-0.77	-1.00	0.00	-6.15
$WM_{unrelated}$	99.38	100	100	100	-0.89	0.02	0.02	0.00	17.22	0.81	90.98	4.00	-0.33	-6.03	-2.94	-6.55
WM_{mark}	97.40	99.64	99.64	94.63	-0.96	-0.16	0.00	-0.20	69.03	97.03	96.97	69.96	-1.21	-8.37	-4.27	-25.07
$WM_{abstract}$	73.00	100	100	100	-0.89	0.09	0.00	0.00	78.00	95.00	97.00	98.00	-0.30	-6.59	-2.38	-7.81
WM_{adv}	91.00	100	100	100	-0.47	-0.46	0.00	-0.21	96.00	7.00	97.00	94.00	-0.34	-5.96	-3.66	-5.61
$WM_{passport}$	80.00	100	71.00	87.00	-0.53	0.20	-1.59	-1.49	84.00	94.00	82.00	91.00	0.00	-2.92	0.00	-2.73
$WM_{encoder}$	96.50	96.94	99.20	98.60	-1.25	-0.02	0.00	-0.82	99.00	91.07	98.20	92.80	-0.57	-4.11	-2.38	-5.69
WM_{exp}	92.00	100	100	100	-0.53	0.17	0.00	0.08	92.00	99.00	98.00	97.00	-2.14	-8.74	-1.81	-5.89
DeepSigns	39.00	89.00	100	98.00	-0.65	-1.99	0.00	-0.62	81.00	98.00	99.00	78.00	-0.45	-4.15	-2.84	-6.24

Table 15: Trigger set recalls of M_{adv} after ownership piracy attacks. Numbers in parentheses denote the differences of trigger set recalls between \mathcal{A} and \mathcal{O} .

	\mathcal{A} 's Trigger Set Recall (%)				\mathcal{O} 's Trigger Set Recall (%)				Δ Test Acc. (%)			
	MN	GT	C10	C100	MN	GT	C10	C100	MN	GT	C10	C100
$WM_{content}$	86.00 (36.24)	99.00 (98.96)	100 (99.72)	100 (99.80)	49.76	0.05	0.28	0.20	-1.34	3.11	-6.32	-13.24
WM_{noise}	92.00 (91.91)	99.00 (74.95)	100 (97.20)	100 (78.00)	0.09	24.05	2.80	22.00	-0.94	3.79	-6.32	-15.20
$WM_{unrelated}$	96.00 (86.72)	98.00 (37.28)	94.00 (43.48)	99.00 (99.00)	9.28	60.72	50.52	0.00	-3.12	4.31	-6.10	-14.28
WM_{mark}	87.00 (75.46)	99.00 (93.38)	98.00 (94.94)	100 (99.32)	11.54	5.62	3.06	0.68	-1.32	2.22	-4.58	-9.20
$WM_{abstract}$	89.00 (61.00)	99.00 (67.00)	98.00 (81.00)	100 (100)	28.00	32.00	17.00	0.00	-1.76	1.63	-5.88	-16.46
WM_{adv}	75.00 (41.00)	91.00 (79.00)	98.00 (92.00)	100 (93.00)	34.00	12.00	6.00	7.00	-1.38	-0.22	-4.74	-11.94
$WM_{passport}$	94.00 (89.00)	0.00 (-6.00)	0.00 (-10.00)	15.00 (14.00)	5.00	6.00	10.00	1.00	-9.66	-9.63	-21.12	-23.34
$WM_{encoder}$	98.00 (88.00)	100 (97.70)	100 (88.20)	100 (99.00)	10.00	2.30	11.80	1.00	-2.00	5.86	-6.48	-15.44
WM_{exp}	70.00 (70.00)	98.00 (98.00)	98.00 (96.00)	100 (100)	0.00	0.00	2.00	0.00	-1.56	4.13	-9.04	-12.38
DeepSigns	93.00 (88.00)	100 (98.00)	99.00 (92.00)	100 (100)	5.00	2.00	7.00	0.00	-2.92	2.37	-4.32	-12.76

Table 16: Trigger set recalls of M_{wm} after ambiguity attacks. Numbers in parentheses denote the differences of trigger set recalls between \mathcal{A} and \mathcal{O} .

	\mathcal{A} 's Trigger Set Recall (%)				\mathcal{O} 's Trigger Set Recall (%)				Δ Test Acc. (%)			
	MN	GT	C10	C100	MN	GT	C10	C100	MN	GT	C10	C100
$WM_{content}$	100 (17.06)	98.00 (98.00)	100 (97.96)	100 (99.20)	82.94	0.00	2.04	0.80	-0.52	-1.68	-3.76	-10.64
WM_{noise}	100 (99.79)	98.00 (38.81)	100 (96.40)	100 (54.40)	0.21	59.19	3.60	45.60	-0.44	-2.15	-4.02	-11.62
$WM_{unrelated}$	98.00 (-1.76)	100 (0.00)	100 (4.74)	97.00 (97.00)	99.76	100	95.26	0.00	-1.08	-0.51	-4.10	-11.08
WM_{mark}	100 (88.43)	100 (94.90)	100 (97.68)	94.00 (93.10)	11.57	5.10	2.32	0.90	-0.82	1.06	-2.18	-6.54
$WM_{abstract}$	100 (59.00)	100 (65.00)	100 (76.00)	100 (98.00)	41.00	35.00	24.00	2.00	-1.02	2.26	-3.90	-11.62
WM_{adv}	100 (77.00)	100 (30.00)	100 (92.00)	100 (89.00)	23.00	70.00	8.00	11.00	-0.84	-1.33	-2.90	-8.36
$WM_{passport}$	100 (93.00)	48.00 (14.00)	0.00 (-19.00)	41.00 (39.00)	7.00	34.00	19.00	2.00	-0.36	5.24	-11.12	-17.62
$WM_{encoder}$	100 (90.33)	99.00 (96.45)	100 (87.40)	100 (98.20)	9.67	2.55	12.60	1.80	-1.28	-1.08	-3.82	-11.76
WM_{exp}	48.00 (47.00)	0.00 (0.00)	100 (98.00)	0.00 (0.00)	1.00	0.00	2.00	0.00	-1.34	2.34	-3.56	-9.40
DeepSigns	100 (90.00)	100 (97.00)	100 (94.00)	98.00 (97.00)	10.00	3.00	6.00	1.00	-1.28	0.67	-2.68	-8.40